The contribution of wood burning and other pollution sources to wintertime organic aerosol levels in two Greek cities

Kalliopi Florou[1,2], Dimitrios K. Papanastasiou[1,2], Michael Pikridas[1,2], Christos Kaltsonoudis[1,2], Evangelos Louvaris[1,2], Georgios I. Gkatzelis[1,2], David Patoulias[1,2], Nikolaos Mihalopoulos[3,4], and Spyros N. Pandis[1,2,5]

[1]Institute of Chemical Engineering Sciences, ICE/FORTH, Patras, Greece,

[2]Department of Chemical Engineering, University of Patras, Patras, Greece,

[3]Department of Chemistry, University of Crete, Greece

[4]IERSD, National Observatory of Athens, Athens, Greece

[5]Department of Chemical Engineering, Carnegie Mellon University, Pittsburgh, USA

Correspondence to: Spyros N. Pandis (spyros@chemeng.upatras.gr)

Abstract. The composition of fine particulate matter (PM) in two major Greek cities (Athens and Patras) was measured during two wintertime campaigns conducted in 2013 and 2012, respectively. A major goal of this study is to quantify the sources of organic aerosol (OA) and especially residential wood burning, which has dramatically increased due to the Greek financial crisis. A high resolution time-of-flight aerosol mass spectrometer (HR-ToF-AMS) was deployed in both sites. PM with diameter less than 1 μm (PM_1) consisted mainly of organics (60-75%), black carbon (5-20%) and inorganic salts (around 20%) in both Patras and Athens. In Patras, during evening hours, PM_1 concentrations were as high as 100 μg m^{-3}, of which 85% were OA. In Athens, the maximum hourly value observed during nighttime was 140 μg m^{-3}, of which 120 μg m^{-3} was OA. 40-60% of the average OA was due to biomass burning for both cities, while the remaining mass originated from traffic (12-17%), cooking (12-16%) and long-range transport (18-24%). The contribution of residential wood burning was even higher (80-90%) during the nighttime peak concentration periods, and less than 10% during daytime. Cooking OA contributed up to 75% during mealtime hours in Patras, while traffic-related OA was responsible for 60-70% of the OA during the morning rush hour.

1. Introduction

Fine particulate matter is associated with premature mortality and cardiovascular disease (Nel,
2005), but also impacts climate, visibility, and ecosystems (Grantz et al., 2003; Hallquist et al.,
2009; Watson, 2002). An important fraction of submicrometer PM is organic representing 20 -
90% of PM_1 mass worldwide (Jimenez et al., 2009; Zhang et al., 2007) and originating from
various anthropogenic and natural sources. Organic aerosol (OA) can be either emitted directly
in particulate form, and is considered primary (POA) or can be produced in the atmosphere by
oxidation of organic gaseous precursors and is considered secondary (SOA) (Kanakidou et al.,
2005; Turpin and Huntzicker, 1995). POA is emitted during combustion of fossil fuels, biomass
burning, cooking, etc. (Hallquist et al., 2009; He et al., 2010; Mohr et al., 2009).

Aerosol mass spectrometry can quantify the mass spectra of OA and helps identify its
sources (Jayne et al., 2000). Source apportionment techniques, such as Positive Matrix
Factorization (PMF), are widely used in order to estimate the contributions of the various OA
sources (Lanz et al., 2007; Mohr et al., 2009; Paatero and Tapper, 1994). Sources that are often
identified include oxygenated OA (OOA), hydrocarbon-like OA (HOA), biomass burning OA
(BBOA), and cooking OA (COA) (Aiken et al., 2009; He et al., 2010; Herndon et al., 2008;
Huang et al., 2011; Mohr et al., 2009; Saarikoski et al., 2012; Zhang et al., 2007).

During wintertime, wood burning for domestic heating purposes is one of the main
sources of OA in several countries (Alfarra et al., 2007; Puxbaum et al., 2007). Biomass burning
is a major source of gas- and particle-phase air pollution on urban (Robinson et al., 2006;
Schauer and Cass, 2000), regional (Watson, 2002; Wotawa and Trainer, 2000) and global (Bond
et al., 2004; Lelieveld et al., 2001) scales. Violations of daily PM standards due to wood burning
have been reported in major European cities such as London, Paris and Berlin (Fuller et al.,
2013; 2014). In several countries while traffic and industrial emissions are decreasing, the impact
of residential wood burning emissions on air quality is increasing (Favez et al., 2010).

In Greece, the use of woodstoves and fireplaces has increased dramatically during the last
few years. Pikridas et al. (2013) reported that biomass burning for heating purposes was the
dominant source of OA during wintertime in Patras, the third biggest city of Greece. Elevated
mass concentrations of $PM_{2.5}$ (diameter less than 2.5 μm), due to wood burning were also
observed in the capital and largest city of Greece, Athens, coinciding with the beginning of the
economic crisis in Greece (Paraskevopoulou et al., 2014). Measurements conducted during 2010
and 2012, in the city of Thessaloniki (Petrakakis et al., 2013) showed an increase of PM_{10}
(diameter less than 10 μm) by 13% and $PM_{2.5}$ by 25% during domestic heating hours. Gaidajis et

al. (2014) reported the same behavior in Northern Greek cities (Kavala and Drama), where the daily average PM_1 concentrations exceeded 40 µg m^{-3}.

In this study, a HR-ToF-AMS was deployed in order to investigate the chemical composition of PM_1 in two Greek cities (Athens and Patras) during two different wintertime periods (2012 and 2013). The PMF source apportionment algorithm, used unconstrained, was applied to the corresponding datasets, estimating the contributions of the different OA sources, without assuming any a priori knowledge of their origin. Previous studies in these areas have relied on filter-based measurements of the $PM_{2.5}$ and PM_{10} concentrations (Argyropoulos et al., 2012; Chaloulakou et al., 2003; Katragkou et al., 2009; Koulouri et al., 2008; Theodosi et al., 2011) and had limited or no information about the composition of the OA. Few PM source apportionment studies are available for Athens. Dall'Osto and Harrison (2006) using an aerosol time-of-flight mass spectrometer (ATOFMS) found two dominant particle types in Athens: calcium-rich dust particles and secondary carbonaceous ones. The main objectives of this paper is to quantify the contribution of wood combustion and the fine PM levels of additional OA sources in the corresponding areas during wintertime.

2.   Experimental Section

2.1   Measurement Sites

Patras: Patras is the third biggest city of Greece with 300,000 inhabitants and is situated at the foothills of Mount Panachaikon, overlooking the Gulf of Patras, 220 km west of Athens. The instruments were housed inside the campus of the Technological Educational Institute (TEI) of Patras (38^{0}13' N, 21^{0}45' E) and were monitoring from February 26 to March 5, 2012. The TEI is in the southwest of the city, surrounded by moderate traffic streets and houses and is considered an urban site (Fig. S1). Measurements of black carbon (BC) were made at the center of the city (38^{0}14' N, 21^{0}44' E), approximately 4 km away from the main site. A more detailed description of the two sites and the instrumentation used can be found in Pikridas et al. (2013).

Athens: Athens is the capital and largest city of Greece, with approximately 5 million inhabitants within the Greater Athens Metropolitan area, which represents almost half of the country's population (Fig. S1). An extensive campaign was conducted in the center of Athens from January 10 till February 9, 2013, the year following the Patras campaign. The measurements took place at the premises of the National Observatory of Athens (NOA) at

Thiseio ($37^0$58' N, $23^0$43' E). NOA is situated on the small hill of the Nymphs (100 m above sea level), overlooking the Acropolis and near the city center of Athens.

100

2.2   Instrumentation

The same instruments and sampling approach were used during both campaigns. More specifically:

HR-ToF-AMS: The Aerodyne Aerosol Mass Spectrometer (AMS), developed by Jayne et

105   al. (2000), can provide continuous quantitative size and composition information for the non-refractory (NR) components of submicron atmospheric aerosol in real time. The chemical composition of NR-PM$_1$ organic and inorganic (nitrate, sulfate, ammonium and partially potassium) aerosol particles was monitored using a High Resolution Time of Flight AMS (HR-ToF-AMS) (Canagaratna et al., 2007; DeCarlo et al., 2006; Drewnick et al., 2005). The sample

110   during this study was not dried, and the vaporizer surface temperature was set at 600 ^{o}C. The HR-ToF-AMS measurements during both campaigns alternated between the V- and W-modes every 3 min, but only the V-mode data are presented here.

SMPS: The ambient aerosol number distribution, for particles smaller than 500 nm in diameter, was measured by a TSI Scanning Mobility Particle Sizer (SMPS) (model 3081)

115   coupled with a Condensation Particle Counter (CPC) (model 3775). The system operated at a sheath flow rate of 5 L min^{-1}, a sample flow rate of 1 L min^{-1}, without drying the sample.

MAAP: PM$_{2.5}$ aerosol absorption was monitored continuously during the two campaigns by a Multi Angle Absorption Photometer (MAAP, Thermo Scientific Inc. model 5012). The MAAP estimates black carbon (BC) mass loadings by combining aerosol optical absorption and back

120   scattering (Petzold and Schönlinner, 2004). The MAAP was set at a wavelength of 637 nm during the measurements and its inlet was heated to 70 ^{o}C.

PTR-MS: The VOCs during the Athens campaign were measured by a PTR-MS (Ionicon Analytik Inc.), the operation principles and application details of which can be found in Steinbacher et al. (2004). Additional information and analysis about these VOC measurements

125   during the sampling period are presented by Kaltsonoudis et al. (2016).

Thermodenuder: The aerosol volatility was quantified using a thermodenuder (TD), based on the design of An et al. (2007). The TD consisted of a heating section in which particles were volatilized, followed by a denuder section, containing activated charcoal to remove the vapors. The air mass passed alternately through the bypass line and the heated section. The TD

130   operated in the temperature range from 25 to 400 ^{o}C with a centerline residence time of 14 s at

25 ℃. A detailed analysis of these measurements is presented in Louvaris et al. (2016) and Gkatzelis et al. (2016).

Gas monitors: The concentrations of CO, CO_2, NO_x and O_3 were measured by the corresponding Teledyne monitors (models 300E, T360, T201 and 400E, respectively).

135   *Filters:* Three different filter samplers were used in order to collect $PM_{2.5}$ samples for the measurement of organic carbon (OC), elemental carbon (EC), water-soluble organic carbon (WSOC) and the main ions. The Met One SuperSASS (Speciation Air Sampler System) was deployed during the Patras campaign, while a dichotomous Partisol sampler (Rupprecht & Patashnick Co., Inc.) and a Partisol FRM (Federal Reference Method) Model 2000 were used in

140   Athens. Both teflon and quartz fiber filters were used in Athens and Patras at daily, 12-hour and 6-hour collection intervals. Details about the filter extraction procedure and chemical analysis can be found in Pikridas et al. (2013) and Paraskevopoulou et al. (2014).

2.3   AMS Data analysis

145   All HR-ToF-AMS data were analyzed using the standard AMS software toolkit (SQUIRREL v1.53) while the high-resolution data were processed using the Peak Integration by Key Analysis (PIKA v1.10C, Sueper, 2011) software within Igor Pro 6.34A (Wave Metrics). For the determination of the elemental ratios measured by the HR-AMS both the method of Aiken et al. (2008) and the improved ambient calculation approach proposed by Canagaratna et al. (2015)

150   were used. In order to calculate the collection efficiency (CE) of the HR-ToF-AMS, we combined the HR-ToF-AMS mass distributions and the SMPS volume distributions (for particle diameters between 10 and 500 nm) applying the algorithm of Kostenidou et al. (2007) every two hours. The algorithm was modified to take into account the BC measured by the MAAP, assuming that the BC had the same size distribution as the OA.

155   PMF analysis (Lanz et al., 2007; Paatero and Tapper, 1994; Ulbrich et al., 2009) was performed using as input the HR-AMS organic mass spectra (*m/z* values 12-200) in order to determine the different OA sources. The mass spectra of the identified factors and those in the literature have been compared using the theta angle (θ) between the corresponding vectors (Kostenidou et al., 2009). This method treats mass spectra signals as vectors in a multi-

160   dimensional space, with size equal to the number of m/z values used. Two spectra are considered to be the same, if the angle theta (θ) between them, is zero. In practice, a low value of the theta angle (less than 10°) indicates high similarity between the two spectra. This approach has been

utilized by commercially available software to match unknown mass spectra with references
from mass spectral libraries (Stein and Scott, 1994). For the comparison of the OOA and HOA

165   spectra with the ones in the literature, only HR spectra using the fragmentation table by Aiken et
al. (2009) were used. The BBOA and COA spectra have been compared with almost all the
corresponding spectra found in the database (both HR and unite mass resolution), resulting in
higher theta values due to differences at m/z 18, 28, and 39.

170   **3. Meteorology**

During the Patras campaign, the ambient temperature ranged from 4 ^{o}C to 16 ^{o}C, with an average
of 11 ^{o}C. The average RH was 75% (ranging from 40 to 90%) (Figure 1). Three types of air
masses were identified using back trajectory analysis based on FLEXPART (Stohl et al., 2005)
during the campaign (Fig. S2). The periods Feb. 25-26 and March 3-4 were characterized by air

175   masses coming predominantly from western Greece (44% of the air masses). During February
26-27 and March 5 the air masses had marine origin (14%), while air masses during February 28
to March 2 were originating from central Greece and the Balkans (42%). Examples of the three
categories are depicted in Fig. S3.

During the Athens campaign, the average ambient temperature was 12.5 ^{o}C (ranging

180   from 6 ^{o}C to 19 ^{o}C), while the average RH was 71% (ranging from 25 to 95%) (Fig. 2).
FLEXPART indicated four types of air masses arriving at the site. The first type originated from
Africa and passed over the Mediterranean Sea. The second had marine origin coming from the
west often passing over Sicily. The third came from the NE passing over the Aegean and the
Eastern Balkans. Finally, the fourth type included air masses from central Greece and the

185   western Balkans. Examples of these trajectories are depicted in Fig. S4 and a summary of the
meteorological conditions is provided in Fig. S5.

4. PM$_1$ chemical composition and characteristics

4.1 PM$_1$ chemical composition

190   **Patras:** The estimated mean value of the AMS collection efficiency (CE) during the wintertime
campaign in Patras was 0.77±0.05. The density of organics estimated by the same algorithm was
1.45±0.04 g cm^{-3}, which is close to the one for Patras during the summer of 2012 (1.34±0.21 g
cm^{-3}, Kostenidou et al., 2015). The one-hour averaged PM$_1$ mass concentration (estimated as the
sum of the concentration of the AMS and MAAP) varied from a few μg m^{-3} up to more than 100

195   μg m^{-3} (Fig. 1). The average PM$_1$ mass concentration was approximately 25 μg m^{-3} (of which 2

μg m^{-3} was BC and 18 μg m^{-3} was OA). The OA mass concentration increased dramatically during the evening hours, reaching levels up to 85 μg m^{-3}. The OA also increased during the morning rush hour (7:00-10:00 LST), but the corresponding concentrations were less than 25 μg m^{-3}. BC concentrations followed closely the variation of OA, with maximum values around 8 μg

200 m^{-3} during nighttime and 4 μg m^{-3} during rush hour in the mornings. The nitrate mass concentration followed a similar trend with OA with significant peaks occurring both during the morning and evening hours. PM$_1$ nitrate was on average 1 μg m^{-3}, but higher values up to 5 μg m^{-3} were measured during the second half of the campaign (from March 1 to 5). The sulfate concentration was on average 2.6 μg m^{-3} and had smaller fluctuations during the campaign,

205 indicating a different source origin. Chloride's average mass concentration was 0.4 μg m^{-3}, but reached values up to 7 μg m^{-3} (March 4). The ammonium concentration followed closely that of sulfate, chloride, and nitrate, indicating the formation of the corresponding ammonium salts.

Athens: The mass concentrations of OA, sulfate, nitrate, ammonium, chloride, and BC are

210 depicted in Fig. 2. The dominant component of PM$_1$ was OA (61%). The average AMS CE during the campaign calculated by the Kostenidou et al. (2007) algorithm was 0.85±0.23 and the density of OA was 1.29±0.21 g cm^{-3}. A similar OA density was estimated for Athens during the summer of 2012 (1.15±0.36 g cm^{-3}, Kostenidou et al., 2015). During the wintertime campaign in Athens, the average total PM$_1$ mass concentration was approximately 10 μg m^{-3} (of which, 2 μg

215 m^{-3} was BC), while the hourly maximum value was 140 μg m^{-3} (of which 120 μg m^{-3} was OA). OA was the major component of PM$_1$ with frequent nighttime (after 18:00 LST) peaks exceeding 40 μg m^{-3} (Fig. 2). During most campaign days PM$_1$ was lower than 20 μg m^{-3} due to frequent rain and strong winds (Fig. S6). BC during the nighttime was as high as 15 μg m^{-3}, while the corresponding morning rush hour maximum was 8 μg m^{-3}. Average ammonium mass

220 concentration was low and around 0.4 μg m^{-3}, while the average sulfate was 0.96 μg m^{-3}. The nitrate was on average 0.48 μg m^{-3}, but its maximum values were up to 3.4 μg m^{-3} during nighttime. The correlation between OA and nitrate was moderate (R^2=0.59).

During the high mass concentration days, and between 18:30 to 02:30 LST, OA was highly correlated (R^2=0.95) with acetonitrile (PTR-MS, *m/z* 42, CH$_3$CN$^+$), indicating that

225 biomass burning was the dominant OA source during these hours. As a reference, during the remaining period the correlation between OA and acetonitrile deteriorated to R^2=0.54. During the same hours, isoprene (PTR-MS, *m/z* 69) and benzene (PTR-MS, *m/z* 79) both constituents of petrol fuel (Borbon et al., 2001), were also correlated (R^2=0.93 and R^2=0.95, respectively) with

OA, and also with each other (R^2=0.95). Both compounds are emitted to the atmosphere by
230   transportation sources (Langford et al., 2009).

Diurnal profiles: The average diurnal profiles of the main PM_1 species during the two
campaigns are shown in Fig. 3. In Patras, the average OA and BC concentrations were
characterized by two major peaks during the day (Fig. 3). The first one appeared at around 8:00
235   LST coinciding with the morning rush hour traffic, while the second one, which was
approximately two times higher for both OA and BC, at 20:00 LST. During the evening the OA
and BC concentrations increased considerably, and were responsible for almost 90% of the total
measured PM_1 mass, until around midnight. Sulfate had a relatively flat diurnal profile, while
nitrates had two peaks, which coincided with those of OA and BC. This suggests that nitrate and
240   OA had at least to some extent, similar sources. The diurnal variation of chloride had a major
morning peak at around 7:00 LST. This could be due to two Olympic-size swimming pools,
located in a major athletic center, less than 1 km from the sampling site, since the peak coincides
with their opening and cleaning hours. There was also an evening chloride peak (20:00 LST)
coinciding with the peak of OA.

245   In Athens, the OA average diurnal profile was dominated by an evening peak at around
23:00 LST, almost three hours later than in Patras campaign. BC exhibited two major peaks, one
in the morning at 8:00 LST, which was attributed to the morning rush hour, and another one in
the evening at 23:00 LST, coinciding with the OA peak (Fig. 3). This suggests that OA and BC
probably originated from the same source during the night. Nitrate also displayed two peaks, one
250   in the morning (9:00 LST) during the peak traffic hours, and another one in the late evening
(23:00 LST). Chloride and ammonium exhibited an evening peak at 23:00 LST, while sulfate
had once more a rather flat average diurnal profile.

Size distributions: The average size distributions of the different aerosol species (sulfate,
255   organics, ammonium, chloride and nitrate) as a function of the vacuum aerodynamic diameter
are depicted in Fig. S7. In Patras, sulfate peaked at 340 nm, whereas OA peaked at 140 nm,
implying that the PM_1 particles during the sampling period had different composition at different
size ranges. The size distribution of ammonium mainly followed that of sulfate, contrary to
nitrate, which followed that of OA suggesting that a major fraction of nitrate was in the form of
260   organonitrates (ON). In Athens, the sulfate size distribution peaked at 310 nm, close to value

during the Patras campaign, whereas OA at 250 nm. Nitrate peaked at the same diameter (250 nm) as OA.

4.1.1 Organonitrates

265   The NO_2^+/NO^+ ratio was used in order to estimate the concentration of particulate organonitrates (ON) (Farmer et al., 2010; Fry et al., 2009). Typical values of NO_2^+/NO^+ for NH_4NO_3 have been reported to be in the range from 0.33 to 0.85 (Alfarra et al., 2006; Cottrell et al., 2008; Fry et al., 2009), while those for organonitrates from 0.07 to 0.1 (Fry et al., 2009; Hao et al., 2014). In this work, the measured NO_2^+/NO^+ ratio for pure NH_4NO_3 in Athens and Patras was equal to 0.59

270   and 0.75, respectively. The fraction of ON to the total nitrate was estimated using the equation suggested by Farmer et al. (2010). The minimum observed NO_2^+/NO^+ ratio during each campaign was 0.04 for Athens and 0.055 for Patras. The average ON fraction of the total nitrate in Athens and Patras was 42±25% and 45±14%, respectively. ON are also known to be components of SOA (Farmer et al., 2010; Fry et al., 2009; Ng et al., 2008). In Athens, during

275   nighttime (17:00 till 3:00 LST), the average ON fraction was 38±20%, while during nights (from 20:00 till 3:00 LST) with OA exceeding 15 μg m^{-3} the ON fraction was lower and equal to 19±10%. This suggests that during biomass burning events ON is not the major component of nitrate. In Patras, the average ON fraction during evening peaks (16:00 till 24:00 LST, for the whole dataset) was 36±13%.

280

4.2 OA elemental ratios

The atomic oxygen-to-carbon ratio (O:C) of OA is a useful metric of its extent of oxygenation, which increases as the aerosol is exposed to atmospheric oxidants (Murphy et al., 2011; Sage et al., 2008). In Patras, the average O:C ratio was 0.42±0.09 following the Canagaratna et al.

285   (2015) approach, while the hydrogen-to-carbon ratio (H:C) was 1.71±0.06. For comparison with literature, the corresponding values following the Aiken et al. (2008) approach were 0.33±0.07 and H:C=1.53±0.05. The corresponding time series are shown in Figs. S8 and S9. In Athens, the average O:C ratio based on the Canagaratna approach was 0.32±0.11 (0.26±0.09 for the Aiken approach) while the H:C was 1.72±0.11 (1.59±0.11 using the Aiken approach). The temporal

290   evolution of these ratios is also depicted in Fig. S8 and Fig. S9. The relatively low average values of O:C for both Athens and Patras are consistent with the OA being dominated by primary emissions (Allan et al., 2010). The corresponding O:C ratios during summertime for Athens and Patras were approximately 0.2 units higher (Kostenidou et al., 2015).

Another metric of the extent of oxidation of atmospheric OA, is the average carbon oxidation state OS_C, a value that increases upon oxidation (Kroll et al., 2011). The OS_C for both cities was calculated by applying the equation proposed by Kroll et al. (2011):

$$OS_c = 2(O:C)-(H:C) \tag{1}$$

In Patras, OS_C was -0.88±0.19, ranging from -1.40 to -0.37 while in Athens, the OS_C was on average -1.08±0.28 varying from -1.8 to 0.98 (Fig. S10).

The average diurnal profiles of O:C, H:C and OS_C for both cities are shown in Fig. 4. In Patras, the O:C ratio increased significantly during the late night hours (2:00 to 7:00 LST), during the morning (peak at around 10:00 LST), and also at around 15:00 in the afternoon. In Athens, the O:C increased during the early morning hours and after 10:00 LST. The diurnal profiles of OS_C were similar to those of O:C. The mean organic-aerosol-to-organic-carbon ratio (OA/OC) for Athens was 1.50±0.1, and varied between 1.2 and 2.2 during the measurement period, while in Patras it was 1.59±0.1, ranging from 1.3 to 2.

5. Source apportionment of OA

Positive matrix factorization (Paatero and Tapper, 1994)(PMF) was applied to the HR-ToF-AMS organic mass spectra (*m/z* up to 200), using the PMF Evaluation Tool, PET (Lanz et al., 2008; Ulbrich et al., 2009). The selection of the PMF solution was based on the comparison of the spectra of the calculated factor to those of the literature, their physical meaning, their diurnal cycles, the correlation of the factor's resulting time-series with each other and other variables (usually concentrations of other pollutants), and finally based on the PMF-model residuals. For both campaigns, biomass burning was identified as the dominant source of OA, and was responsible for 40-60% of the total OA. The results for both cities are summarized in Figure 5.

For Patras, PMF solutions with 1 to 7 factors were investigated. In the three factor solution a BBOA, a HOA and an OOA factor were obtained, with BBOA being the dominant component of OA. Moving to a 4-factor solution, a second factor related to biomass burning was obtained quite different from the other, with a noticeable difference in both fractions of *m/z* 44 and 60 (f_{44} and f_{60}), and a high value of theta angle ($\theta=32^{o}$) between the mass spectra. In the five-factor solution, a COA factor was added. The increase in the number of factors up to this point was accompanied by a reduction in the residuals. On the other hand, the model residuals for the 6 and 7-factor solutions were almost identical to those of the 5-factor solution. Thus, a 5-factor solution was selected for the specific dataset (SI, Section 7, Figures S11-S17). The two biomass burning-related OA factors (BBOA-I and BBOA-II) dominated the measured OA composition

(almost 60%) during the evenings. The OOA factor accounted on average for 18% of the OA, while HOA and COA represented 12% and 11%, respectively. The BBOA, HOA and COA factors correspond to primary sources, whereas the OOA to atmospheric processing (secondary OA). The PMF factors' time series and contribution to PM_1 OA are depicted in Fig. 6.

In Athens the PMF model identified four sources of OA: BBOA (43%), OOA (24%), HOA (17%) and COA (16%). Their time series and contribution to PM_1 OA are depicted in Fig. 7. A PMF analysis with up to 6 factors was performed (SI, Section 7, Figures S18-S24). By extending the solution from a 4 to a 5-factor solution, another biomass burning-related (BBOA-1, 14% of OA) factor was generated in addition to the first one (BBOA, 39% of OA). The PMF residuals in this case decreased slightly and only for the two first days of the campaign (Fig. S19). For this solution, the mass concentrations of OOA (20% of OA), HOA (13% of OA), and COA (14% of OA) were pretty similar to those in the 4-factor solution. The 5-factor solution was not used because the two biomass burning factors resembled each other ($\theta=15^{\circ}$) and had similar diurnal profiles.

Figure 8 summarizes the mass spectra of the identified OA components. Each one of these is analyzed in the following sections.

5.1 Biomass Burning-related Organic Aerosol

Patras: The selected five-factor PMF solution for Patras included two BBOA-like factors named BBOA-I and BBOA-II. Both of these factors had significant contributions at the m/z values 60 ($C_2H_4O_2^+$) and 73 ($C_3H_5O_2^+$), that are typical fragments of levoglucosan, a marker for biomass burning (Aiken et al., 2009; Alfarra et al., 2007; Cubison et al., 2011; Heringa et al., 2011). However, their mass spectra were quite different ($\theta=32^{\circ}$) and their time series had a rather low correlation to each other ($R^2=0.2$). The two BBOA factors represented 60% of the OA on average during the campaign with their contribution rising to 90% or so during the night hours (18:00 to 24:00 LST). The fraction of m/z 60, characteristic of levoglucosan, was $f_{60}=0.025$ in BBOA-I and much lower, $f_{60}=0.009$, in BBOA-II.

The BBOA-I factor was by far the most important component of PM_1 OA (40%) in Patras with a mean concentration of 7 $\mu g\ m^{-3}$. BBOA-I levels increased after 16:00 LST, reaching values exceeding 35 $\mu g\ m^{-3}$ at around 20:00 LST (Fig. 6). During the evening periods it represented up to 75% of the total OA while during the day its concentration was always less than 5 $\mu g\ m^{-3}$. The BBOA-I factor correlated well with the AMS K^+ ($R^2=0.76$), and had modest correlations with the AMS total nitrate ($R^2=0.55$), CO ($R^2=0.40$), and BC ($R^2=0.27$).

360   BBOA-II was the second biomass burning-related factor, contributing 19% to the PM_1 OA in Patras. Its contribution was higher during the first days when it represented up to 40% of the total OA. Its mean value for the whole campaign was equal to 3.3 μg m^{-3}, and its hourly maximum value almost 21 μg m^{-3}. BBOA-II correlated poorly with all the major AMS species ($R^2 < 0.1$) and BC ($R^2 = 0.26$). Its diurnal cycle exhibited two evening peaks, one at 18:00 (LST)

365   and a smaller one at 22:00 (LST). Its mean mass concentration during daytime was less than 3 μg m^{-3}, and close to the corresponding one of BBOA-I.

The BBOA-I and BBOA-II spectra for Patras are shown in Fig. 8. The BBOA-I spectrum had strong signals at m/z 29 (CHO^+), 43 ($C_2H_3O^+$), 60 ($C_2H_4O_2^+$) and 73 ($C_3H_5O_2^+$), while the spectrum of BBOA-II was characterized by lower signal in m/z values attributed to fresh OA,

370   like 43, 55 and 57, and a stronger signal at m/z 44, which is usually related to aged organic aerosol (f_{44} was equal to 0.043). The contribution of m/z 60 in the BBOA-II spectrum was 67% lower compared to the BBOA-I spectrum, suggesting the evaporation of levoglucosan. There was also a prominent peak at m/z 39 as well as a peak at m/z 91, which can be indicative of aromatic species such as benzyl ions (Allan, 2003; Allan et al., 2004; Trainer et al., 2012). This

375   m/z 91 peak was also present in the spectrum of the BBOA factor from the burning of olive tree branches in Greece (Kostenidou et al., 2013). The O:C ratio of BBOA-I was 0.3 while that of BBOA-II was equal to 0.26. The corresponding OA/OC ratios were 1.55 and 1.47. These two factors could correspond to different degrees of aging of the BBOA, different types of combustion or fuel, or a combination of these.

380

Athens: The biomass burning OA (BBOA) factor contributed almost half (43%) of the OA in Athens. BBOA reached hourly levels up to 80 μg m^{-3} during the evening of the first day of the campaign, which was the coldest day during the period of the measurements. The average BBOA concentration was 2.3 μg m^{-3}. However, when meteorological conditions were favorable

385   (no precipitation), BBOA sharply increased after 17:00 LST, frequently reaching values greater than 20 μg m^{-3} at approximately 23:00 LST (Fig. 7). This peak was observed a few hours later in Athens than in Patras, potentially due to the different lifestyles in the two cities. A peak was also observed between 1:00 and 4:00 LST. A similar peak was present in the diurnal profile of the AMS K^+ (Fig. S25), implying a common source for both. This could be due to either morning

390   combustion or vertical mixing. During the rest of the day the BBOA levels remained lower than 1 μg m^{-3}.

BBOA and gas-phase acetonitrile (PTR-MS, m/z 42, CH_3CN^+) were strongly correlated (R^2 =0.81). BBOA was also well correlated with AMS chloride (R^2=0.88). Moderate correlations were observed with CO (R^2=0.58), AMS K^+ (R^2 =0.40), BC (R^2=0.33) and NO_x (R^2=0.29). High

395   correlations were observed between BBOA and 2-methyl-3-buten-2-ol (MBO) (PTR-MS, m/z 87) (R^2=0.93) which is related with emissions from pine trees (Vlasenko et al., 2009), isoprene and furan at m/z 69 (C_5H^+ and $C_4H_5O^+$) (R^2=0.88), methacrolein and methyl vinyl ketone ($C_4H_7O^+$) at m/z 71 (R^2=0.81), and m/z 85 (among possible candidates, ethyl vinyl ketone) (R^2=0.9). These results are consistent with previous studies suggesting that wood burning is

400   major source of biogenic VOCs (Akagi et al., 2011). The correlation between the BBOA factor in Athens and VOCs as measured by the PTR-MS are shown in Table 1.

The AMS spectrum of BBOA in Athens had prominent peaks at m/z 39 ($C_2H_2^+$), 60 ($C_2H_4O_2^+$) and 73 ($C_3H_5O_2^+$). A high contribution to the total organic signal was present at m/z 29 mostly due to CHO^+, consistent with the findings of Alfarra et al. (2007). The BBOA high

405   resolution (HR) spectra, with the dominant ion families are represented in Fig. 8. The BBOA O:C ratio in Athens was 0.27.

BBOA factor comparisons: The mass spectra of BBOA in Athens and BBOA-I in Patras had some similarity (θ=14°) with main differences at m/z 29, 39, 43, 57, 60 and 73 (Fig. S26). Their

410   f_{44} were close to each other (0.02). The mass spectra of BBOA in Athens and BBOA-II in Patras were quite different (θ=25°). Their major differences were presented at m/z values 26, 28, 29, 39, 41, 43, 44, 55, 57, 60, and 73.

The BBOA-I spectrum in Patras was similar to that for Fresno (θ=11°) (Ge et al., 2012), and to BBOA from the MILAGRO campaign (θ=14°)(Aiken et al., 2009) (Fig. S27). The

415   BBOA-II spectrum in Patras was quite different (angles θ exceeding 24°) than those in the literature (Fig. S28). Calculation of the theta angle between the spectrum of BBOA-II and HR spectra of OOA factors revealed lower theta values (less than 30°) between these two types of spectra (Fig. S29), than between BBOA-II and other BBOA spectra, indicating a moderate resemblance of BBOA-II and chemically aged aerosol. The theta angle was lower than 30° with

420   the spectra of OOA in Fresno (Ge et al., 2012), New York (Sun et al., 2012), and SV-OOA from SOAR (Docherty et al., 2011).

The Athens BBOA spectrum was similar (θ=12°) to that of the BBOA factor in Fresno (Ge et al., 2012), had some similarity with spectra from the burning of ponderosa pine duff

425   (θ=21°) and the Alaska core Tundra duff (θ=22°) during FLAME-I (Sullivan et al., 2008). For the rest of the database spectra, the theta angle values exceeded 25° (Fig. S30).

5.2 Oxygenated Organic Aerosol (OOA)

OOA is often considered as a surrogate for secondary OA due to both local production processes and long range transport of chemically aged OA from other areas.

430

Patras: The OOA factor dominated daytime OA and its mass concentration increased during the last days of the campaign. The mean OOA was 3.2 µg m^{-3}, while its hourly maximum value, around midday of March 5, was equal to 10.8 µg m^{-3}. It represented 18% of the OA on average. For comparison, during summertime at the same area, OOA accounted for almost 80% of OA

435   due to the higher photochemical activity (Kostenidou et al., 2015). The average diurnal pattern of OOA was relatively stable (Fig. 9) with small peaks during the morning (8:00 and 11:00 LST) and a little lower values after 18:00 LST. This pattern is consistent with a regional source and domination by atmospheric transport rather than local sources and processes The OOA was correlated reasonably well with particulate ammonium (R^2=0.61) and sulfate (R^2=0.56), while its

440   correlation to nitrate was moderate (R^2=0.38).

Athens: In contrast to other measurement datasets in Athens, in which two OOA types were obtained by PMF (a very oxidized OA, V-OOA, and a moderately oxygenated, M-OOA) (Kostenidou et al., 2015), only one type was clearly present in Athens during the winter. The

445   OOA factor dominated OA during the daytime and its mass concentration increased after January 28, when air masses originated from the Balkans and not from the Mediterranean Sea (SI, Sections 3 and 4). The average OOA concentration was 1.3 µg m^{-3}, with a maximum value of 9.7 µg m^{-3}. OOA was correlated with NH$_4^+$ (R^2=0.65), SO$_4^{2-}$ (R^2=0.58), and NO$_3^-$ (R^2=0.67). The average diurnal concentration of OOA decreased smoothly during morning hours, reaching a

450   minimum at around 15:00 LST, and increased again during the afternoon and evening, peaking at midnight (Fig. 9). This behavior could be due to nighttime SOA production from biomass burning-related VOCs such as monoterpenes (C$_{10}$H$_{16}$), and isoprene (C$_5$H$_8$) reacting with NO$_3$ radicals (Hodzic et al., 2009; Ng et al., 2008; Rollins et al., 2009).

     In Patras, the wintertime OOA O:C ratio was 0.65 (Fig. 10). For comparison reasons, the

455   O:C ratio for V-OOA, M-OOA and b-OOA during the summer campaign of 2012 in Patras, were 0.81, 0.54 and 0.48, respectively (Kostenidou et al., 2015). In Athens, the O:C ratio for OOA

during the winter of 2013 was equal to 0.47 (Fig. 10). The corresponding values of O:C during summertime in Athens, for V-OOA and M-OOA were 0.68 and 0.56, respectively (Kostenidou et al., 2015).

460

OOA factor comparisons: Both OOA spectra were characterized by a strong peak at m/z 44 (mostly due to CO_2^+), related to the thermal decomposition of organic acids (Alfarra et al., 2004), a lower one at m/z 43 (mostly due to $C_2H_3O^+$), and another one at m/z 28, all consistent with the OOA spectra reported in other studies. The OOA spectra in the two cities were quite similar to each other ($\theta=11^o$), with the greater differences at m/z values 28 and 44. The OOA in Athens exhibited lower f_{44} (0.12) compared to the one in Patras (0.15).

The spectrum of OOA in Patras was quite similar to the OOAa and OOAb ($\theta=7^o$) for Po Valley (Saarikoski et al., 2012), the summertime spectra of moderate oxygenated OA (M-OOA) in Athens and Patras ($\theta=10^o$) (Kostenidou et al., 2015), and the LV-OOA spectra ($\theta=11^o$) from both the DAURE (Mohr et al., 2012) and SOAR campaigns (Docherty et al., 2011). Higher theta angles ($\theta=20-40^o$) were found when comparing it to spectra of SV-OOA (Fig. S31) from different studies, implying that the OOA in Patras was closer to LV-OOA, instead of SV-OOA.

The spectrum of OOA in Athens was similar to both the M-OOA identified in Athens ($\theta=8^o$) and Patras ($\theta=10.6^o$) during the summer (Kostenidou et al., 2015). It was also similar with the proposed biogenic OOA factor (b-OOA) ($\theta=10^o$) in Patras for the same summer period, and all the OOA (OOA-a, OOA-b, OOA-c) factors ($\theta=11-13^o$) identified in Po Valley (Saarikoski et al., 2012). The values of the theta angles between the OOA spectra in this study and spectra in the literature are summarized in Figure S31.

5.3 Hydrocarbon-Like Organic Aerosol (HOA)

Athens: The HOA mean value was 0.95 $\mu g\ m^{-3}$, and its hourly maximum concentration was 34 $\mu g\ m^{-3}$. HOA was correlated with CO ($R^2=0.69$) and NO_x ($R^2=0.74$), suggesting that traffic was a major HOA source. HOA was also correlated to AMS chloride ($R^2=0.75$), and VOCs, such as methacrolein (MACR) (PTR-MS, m/z 71) ($R^2=0.74$), naphthalene (PTR-MS, m/z 129) ($R^2=0.73$), benzene (PTR-MS, m/z 79) ($R^2=0.65$), and the xylenes (PTR-MS, m/z 107) ($R^2=0.7$). The HOA correlation with BC for the whole campaign was low ($R^2=0.15$). However, splitting the BC and HOA time series into two periods, one during the day (6:00-18:00 LST) and another one during the night (18:00-6:00 LST), led to high correlation during daytime ($R^2=0.78$) and low during the nighttime ($R^2=0.15$). A potential explanation of this behavior is that BC originated mainly from

490   diesel combustion sources during the day, while during the night it was associated with both traffic and wood burning. The average diurnal pattern of HOA in Athens was the same as that of BC (Fig. S34), and exhibited strong morning (8:00-9:00 LST) and evening peaks (20:00-23:00 LST) consistent with increased traffic during morning and evening rush hours.

495   **Patras:** HOA contributed on average approximately 10% to the total OA, while the corresponding HOA contribution during summer was 7% (Kostenidou et al., 2015). Its mean concentration was 2.1 μg m^{-3}, and its hourly maximum value was 15.8 μg m^{-3}. The strongest peak in the average diurnal cycle occurred in the morning (06:00–09:00 LST) and was probably associated with traffic emissions (Fig. 9). A peak in the afternoon (17:00–22:00 LST) was also

500   present, but was frequently smaller. The time series of HOA showed poor correlation with NO$_x$ ($R^2 = 0.16$), and BC ($R^2 = 0.2$). Splitting again the BC and HOA time series into two periods, one during 4:00-16:00 LST, and another one during 16:00-4:00 LST, led to a higher correlation during the first period ($R^2 = 0.48$). However, no perfect correlation was expected, as the MAAP was monitoring 4 km away from the HR-ToF-AMS.

505   In Athens, the O:C for HOA was equal to 0.13, while its H:C ratio was 1.74. In Patras, the O:C ratio was 0.1, while the H:C ratio was equal to 1.83. The corresponding values of O:C during summertime of 2012 were 0.07 (Athens) and 0.1 (Patras) (Kostenidou et al., 2015).

    HOA factor comparisons: The two HOA spectra were also quite similar to each other (θ=13°)

510   having characteristic peaks at *m/z* 41, 43, 55, 57, 69, 71, 83 and 85 etc., with little signal at *m/z* 44 (Fig. S26). Their major differences were observed at *m/z* 28, 43, 44, 57, 69, and 71, which were generally higher in Patras. The f_{44} in the Athens spectrum was two times higher (0.04) compared to the Patras one. These mass spectra of HOA are similar to those of diesel exhaust (Canagaratna et al., 2004; Schneider et al., 2005), and other incomplete combustion sources.

515   Comparing the identified HOA spectra with literature values, the spectrum of HOA in Athens was similar (θ=6°) with the corresponding one from HOA in Patras during summertime (Kostenidou et al., 2015), and relatively similar with the majority of the other HOA spectra in the literature (Aiken et al., 2009; Crippa et al., 2013; Ge et al., 2012; Saarikoski et al., 2012; Sun et al., 2011) (θ=10-15°), as presented in Fig. S32. The spectrum of HOA in Patras was very

520   similar (θ=5-8 ^{o}) with the spectra of HOA in New York City (Sun et al., 2012), Fresno (Ge et al., 2012), and the MILAGRO campaign (Aiken et al., 2009).

5.4 Cooking Organic Aerosol (COA)

Patras: The COA factor identified during the campaign had a mean value of 2.1 μg m^{-3}, and an hourly maximum value of 33.6 μg m^{-3}. The diurnal profile of COA in Patras exhibited two peaks during the day. The major peak occurred in the late evening (18:00–24:00 LST) probably modulated by the boundary layer height, and a second significant peak around midday (10:00–15:00 LST), both corresponding to typical Greek mealtimes (Fig. 9). Its contribution was similar to that of HOA.

Athens: In Athens, COA exhibited strong night peaks at around 23:00 LST, with values up to 15 μg m^{-3}. Its mean value was 0.9 μg m^{-3}. COA correlated moderately with BC (R^2=0.32), and CO (R^2=0.27), while the correlation between COA and individual VOCs measured by the PTR-MS was relatively poor, with R^2 varying from 0.01 to 0.32. The temporal trend of COA in Athens is different from those in previous studies. Contrary to what was expected, no peak was found during lunch hours (12:00-15:00 LST). However, no other factor displayed a peak during these hours because of the meteorology (strong winds). A large nighttime peak, clearly affected by the decrease of the planetary boundary layer was present at around 23:00 LST (Fig. 9). This late peak is consistent with the late dinner hours of Athenians.

In Patras, the COA O:C ratio was 0.14, while the H:C ratio was equal to 1.71. In Athens, the O:C was 0.11, while the H:C was equal to 1.68. The corresponding values of COA O:C during summertime of 2012 were 0.21 (Athens) and 0.24 (Patras) (Kostenidou et al., 2015).

COA factor comparisons: The COA spectrum, like the HOA one was characterized by the ion series $C_nH_{2n-1}^+$, but also by $C_mH_{2m-1}CO^+$ (*m/z* 41, 55, 69, 83, etc.) and $C_mH_{2m+1}CO^+$ (*m/z* 29, 43, 57, 71, 85, etc.) (Crippa et al., 2013; He et al., 2010) (Fig. 10a). The COA spectra in both cities had some similarity to the HOA spectra but were dominated by *m/z* 41 and 55 instead of *m/z* 43 and 57. The signal of *m/z* 55 in the COA spectrum in Patras was almost twice that of the *m/z* 57. This characteristic of the COA spectrum was first reported by Lanz et al. (2007) and is related to charbroiling (Allan et al., 2010). The COA mass spectra in the two cities were very similar to each other with a theta angle of 8º, and minor differences at *m/z* 27, 28, 39, 41 and 43 (Fig. S26). The COA spectrum in Athens and Patras were rather similar to the COA spectra reported in Fresno (Ge et al., 2012), New York City (Sun et al., 2012) and Paris (Crippa et al., 2013) with theta angles values varying between 11-17º (Fig. S33). Comparing the identified COA spectra

555   with the corresponding ones (called HOA-2) in Athens and Patras during summertime
(Kostenidou et al., 2015), theta values higher than 20 $^{\circ}$ were observed.

6. Conclusions

An aerosol mass spectrometer (HR-ToF-AMS) accompanied by a suite of aerosol and gas related

560   instruments were used for the characterization of the OA in two of the biggest cities of Greece
(Athens and Patras), during two consecutive winter periods (2012 and 2013). The carbonaceous
PM (BC+OA) accounted for about 80% of the measured PM_1 during the two field campaigns,
and up to 95% during morning (5:00-10:00 LST) and evening (16:00-24:00 LST) hours.

During both wintertime campaigns, domestic wood burning was in general a more

565   significant OA source than traffic. The PM_1 consisted of biomass burning-related OA (25-42%),
a contribution from traffic (BC =7-20% and HOA=9-10%), cooking activities (COA= 8-9%),
and also oxygenated OA (OOA=13-15%). Sulfates, ammonium and nitrate accounted for 10%,
4% and 5%, respectively, of the total PM_1 in both cities. The OA O:C ratio for the Athens
campaign was equal to 0.32, while in Patras 0.42, suggesting that the atmosphere in Athens had

570   higher contributions on average by less processed emissions.

Biomass burning related factors were the dominant source (40-60%) of OA in both cities,
and their mass concentration levels increased sharply during the evening hours (18:00- 24:00
LST). The BBOA-I in Patras reached its maximum value at 20:00 LST, three hours earlier than
the BBOA factor in Athens. A second biomass burning-related factor (BBOA-II) was also

575   identified in Patras. The BBOA-II (19% of OA) had a quite different mass spectrum than the
dominant BBOA-I factor. The two BBOA factors (BBOA-I and BBOA-II) exhibited different
diurnal profiles, but comparable O:C ratios (0.30 and 0.26). In Athens, only one BBOA factor
was identified by the PMF analysis.

In both sites the HOA factor had two peaks during morning (8:00-9:00 LST) and evening

580   (20:00-23:00 LST) hours respectively. Its diurnal pattern in Athens followed closely that of BC,
exhibiting strong peaks consistent with increased traffic during morning and evening rush hours.
The two HOA spectra were quite similar to each other (θ=13°) and to the corresponding spectra
reported in campaigns in New York City, Fresno, and Mexico City.

The diurnal profile of COA in Athens exhibited strong peaks only during the night at

585   around 23:00 LST, while COA in Patras exhibited two major peaks during the day (13:00 and
22:00 LST). The two COA mass spectra were very similar to each other with a theta angle of 8°
and also quite similar to COA spectra in Fresno, New York City, and Paris.

The OOA factor dominated daytime OA in both sites and correlated reasonably well with inorganic compounds. In comparison to summertime campaigns in the same cities during 2012,

590 only one type of OOA was present during wintertime. The spectra of OOA in the two cities were quite similar ($\theta=11^{o}$) to each other, and were quite comparable ($\theta=8\text{-}11^{0}$) to the more oxygenated OA (M-OOA) identified during the summertime study.

Both measurement campaigns were conducted during relatively warm wintertime periods. The average ambient temperature for both campaigns was close to 12°C, ranging from

595 6-19 °C in Athens, and 4-16°C in Patras. The contribution of wood burning is expected to be even higher for lower temperatures.

Acknowledgments. The authors would like to acknowledge Dr. Evangelia Kostenidou for her guidance and advice, and also Prof. A. Papalou from the Technological Educational Institute

600 (TEI) of Patras and Dr. E. Gerasopoulos from the Institute of Environmental Research and Sustainable Development (IERSD) of the National Observatory of Athens (N.O.A), for providing the space during the Patras and Athens measurements, respectively. This research was supported by the European Research Council Project ATMOPACS (Atmospheric Organic Particulate Matter, Air Quality and Climate Change Studies) (Grant Agreement 267099), the

605 ESF-NRSF ARISTEIA grant ROMANDE and the Greek/European Union operational program THALES: "Identify sources and physicochemical properties of fine and ultrafine suspended aerosol particles that affect the regional climate of Greece".

References

610 Aiken, A. C., Decarlo, P. F., Kroll, J. H., Worsnop, D. R., Huffman, J. A., Docherty, K. S., Ulbrich, I. M., Mohr, C., Kimmel, J. R., Sueper, D., Sun, Y., Zhang, Q., Trimborn, A., Northway, M., Ziemann, P. J., Canagaratna, M. R., Onasch, T. B., Alfarra, M. R., Prevot, A. S. H., Dommen, J., Duplissy, J., Metzger, A., Baltensperger, U. and Jimenez, J. L.: O/C and OM/OC ratios of primary, secondary, and ambient organic aerosols with high-

615 resolution time-of-flight aerosol mass spectrometry., Environ. Sci. Technol., 42, 4478–4485, 2008.

Aiken, A. C., Salcedo, D., Cubison, M. J., Huffman, J. A., DeCarlo, P. F., Ulbrich, I. M., Docherty, K. S., Sueper, D., Kimmel, J. R., Worsnop, D. R., Trimborn, A., Northway, M., Stone, E. A., Schauer, J. J., Volkamer, R. M., Fortner, E., de Foy, B., Wang, J.,

620 Laskin, A., Shutthanandan, V., Zheng, J., Zhang, R., Gaffney, J., Marley, N. A., Paredes-Miranda, G., Arnott, W. P., Molina, L. T., Sosa, G. and Jimenez, J. L.: Mexico City aerosol analysis during MILAGRO using high resolution aerosol mass spectrometry at the urban supersite (T0) – Part 1: Fine particle composition and organic source

    apportionment, Atmos. Chem. Phys., 9, 6633–6653, doi:10.5194/acp-9-6633-2009, 2009.

625 Akagi, S. K., Yokelson, R. J., Wiedinmyer, C., Alvarado, M. J., Reid, J. S., Karl, T., Crounse, J. D. and Wennberg, P. O.: Emission factors for open and domestic biomass burning for use in atmospheric models, Atmos. Chem. Phys., 11, 4039–4072, doi:10.5194/acp-11-4039-2011, 2011.

    Alfarra, M. R., Coe, H., Allan, J. D., Bower, K. N., Boudries, H., Canagaratna, M. R., Jimenez,
630 J. L., Jayne, J. T., Garforth, A. a., Li, S.-M. and Worsnop, D. R.: Characterization of urban and rural organic particulate in the Lower Fraser Valley using two Aerodyne Aerosol Mass Spectrometers, Atmos. Environ., 38, 5745–5758, doi:10.1016/j.atmosenv.2004.01.054, 2004.

    Alfarra, M. R., Paulsen, D., Gysel, M., Garforth, A. A., Dommen, J., Prévôt, A. S. H.,
635 Worsnop, D. R., Baltensperger, U. and Coe, H.: A mass spectrometric study of secondary organic aerosols formed from the photooxidation of anthropogenic and biogenic precursors in a reaction chamber, Atmos. Chem. Phys., 6, 5279–5293, doi:10.5194/acp-6-5279-2006, 2006.

    Alfarra, M. R., Prevot, A. S. H., Szidat, S., Sandradewi, J., Weimer, S., Lanz, V. A., Schreiber,
640 D., Mohr, M. and Baltensperger, U.: Identification of the mass spectral signature of organic aerosols from wood burning emissions., Environ. Sci. Technol., 41, 5770–7, 2007.

    Allan, J. D.: Quantitative sampling using an Aerodyne aerosol mass spectrometer 1. Techniques of data interpretation and error analysis, J. Geophys. Res., 108, 4090,
645 doi:10.1029/2002JD002358, 2003.

    Allan, J. D., Delia, A. E., Coe, H., Bower, K. N., Alfarra, M. R., Jimenez, J. L., Middlebrook, A. M., Drewnick, F., Onasch, T. B., Canagaratna, M. R., Jayne, J. T. and Worsnop, D. R.: A generalised method for the extraction of chemically resolved mass spectra from Aerodyne aerosol mass spectrometer data, J. Aerosol Sci., 35, 909–922,
650 doi:10.1016/j.jaerosci.2004.02.007, 2004.

    Allan, J. D., Williams, P. I., Morgan, W. T., Martin, C. L., Flynn, M. J., Lee, J., Nemitz, E., Phillips, G. J., Gallagher, M. W. and Coe, H.: Contributions from transport, solid fuel burning and cooking to primary organic aerosols in two UK cities, Atmos. Chem. Phys., 10, 647–668, doi:10.5194/acp-10-647-2010, 2010.

655 An, W. J., Pathak, R. K., Lee, B.-H. and Pandis, S. N.: Aerosol volatility measurement using an improved thermodenuder: Application to secondary organic aerosol, J. Aerosol Sci., 38, 305–314, doi:10.1016/j.jaerosci.2006.12.002, 2007.

    Argyropoulos, G., Manoli, E., Kouras, A. and Samara, C.: Concentrations and source apportionment of PM_{10} and associated major and trace elements in the Rhodes Island,
660 Greece., Sci. Total Environ., 432, 12–22, doi:10.1016/j.scitotenv.2012.05.076, 2012.

Bond, T. C, Streets, D. G., Yarber, K. F., Nelson, S. M., Woo, J.-H. and Klimont, Z..: A technology-based global inventory of black and organic carbon emissions from combustion, J. Geophys. Res., 109, D14203, doi:10.1029/2003JD003697, 2004.

Borbon, A., Fontaine, H., Veillerot, M., Locoge, N., Galloo, J. C. and Guillermo, R.: An investigation into the traffic-related fraction of isoprene at an urban location, Atmos. Environ., 35, 3749–3760, doi:10.1016/S1352-2310(01)00170-4, 2001.

Canagaratna, M. R., Jayne, J. T., Ghertner, D. a., Herndon, S., Shi, Q., Jimenez, J. L., Silva, P. J., Williams, P., Lanni, T., Drewnick, F., Demerjian, K. L., Kolb, C. E. and Worsnop, D. R.: Chase studies of particulate emissions from in-use New York City vehicles, Aerosol Sci. Technol., 38, 555–573, doi:10.1080/02786820490465504, 2004.

Canagaratna, M. R., Jayne, J. T., Jimenez, J. L., Allan, J. D., Alfarra, M. R., Zhang, Q., Onasch, T. B., Drewnick, F., Coe, H., Middlebrook, A., Delia, A., Williams, L. R., Trimborn, A. M., Northway, M. J., DeCarlo, P. F., Kolb, C. E., Davidovits, P. and Worsnop, D. R.: Chemical and microphysical characterization of ambient aerosols with the aerodyne aerosol mass spectrometer, Mass Spectrom. Rev., 26, 185–222, doi:10.1002/mas.20115, 2007.

Canagaratna, M. R., Jimenez, J. L., Kroll, J. H., Chen, Q., Kessler, S. H., Massoli, P., Hildebrandt Ruiz, L., Fortner, E., Williams, L. R., Wilson, K. R., Surratt, J. D., Donahue, N. M., Jayne, J. T. and Worsnop, D. R.: Elemental ratio measurements of organic compounds using aerosol mass spectrometry: characterization, improved calibration, and implications, Atmos. Chem. Phys., 15, 253–272, doi:10.5194/acp-15-253-2015, 2015.

Chaloulakou, A., Kassomenos, P., Spyrellis, N., Demokritou, P. and Koutrakis, P.: Measurements of PM_{10} and $PM_{2.5}$ particle concentrations in Athens, Greece, Atmos. Environ., 37, 649–660, doi:10.1016/S1352-2310(02)00898-1, 2003.

Cottrell, L. D., Griffin, R. J., Jimenez, J. L., Zhang, Q., Ulbrich, I., Ziemba, L. D., Beckman, P. J., Sive, B. C. and Talbot, R. W.: Submicron particles at Thompson Farm during ICARTT measured using aerosol mass spectrometry, J. Geophys. Res., 113, D08212, doi:10.1029/2007JD009192, 2008.

Crippa, M., DeCarlo, P. F., Slowik, J. G., Mohr, C., Heringa, M. F., Chirico, R., Poulain, L., Freutel, F., Sciare, J., Cozic, J., Di Marco, C. F., Elsasser, M., Nicolas, J. B., Marchand, N., Abidi, E., Wiedensohler, a., Drewnick, F., Schneider, J., Borrmann, S., Nemitz, E., Zimmermann, R., Jaffrezo, J.-L., Prévôt, a. S. H. and Baltensperger, U.: Wintertime aerosol chemical composition and source apportionment of the organic fraction in the metropolitan area of Paris, Atmos. Chem. Phys., 13, 961–981, doi:10.5194/acp-13-961-2013, 2013.

Cubison, M. J., Ortega, A. M., Hayes, P. L., Farmer, D. K., Day, D., Lechner, M. J., Brune, W. H., Apel, E., Diskin, G. S., Fisher, J. A., Fuelberg, H. E., Hecobian, A., Knapp, D. J., Mikoviny, T., Riemer, D., Sachse, G. W., Sessions, W., Weber, R. J., Weinheimer, A. J.,

Wisthaler, A. and Jimenez, J. L.: Effects of aging on organic aerosol from open biomass burning smoke in aircraft and laboratory studies, Atmos. Chem. Phys., 11, 12049–12064, doi:10.5194/acp-11-12049-2011, 2011.

Dall'Osto, M. and Harrison, R.: Chemical characterisation of single airborne particles in Athens (Greece) by ATOFMS, Atmos. Environ., 40, 7614–7631, doi:10.1016/j.atmosenv.2006.06.053, 2006.

DeCarlo, P. F., Kimmel, J. R., Trimborn, A., Northway, M. J., Jayne, J. T., Aiken, A. C., Gonin, M., Fuhrer, K., Horvath, T., Docherty, K. S., Worsnop, D. R. and Jimenez, J. L.: Field-deployable, high-resolution, time-of-flight aerosol mass spectrometer., Anal. Chem., 78, 8281–9, doi:10.1021/ac061249n, 2006.

Docherty, K. S., Aiken, A. C., Huffman, J. A., Ulbrich, I. M., DeCarlo, P. F., Sueper, D., Worsnop, D. R., Snyder, D. C., Peltier, R. E., Weber, R. J., Grover, B. D., Eatough, D. J., Williams, B. J., Goldstein, A. H., Ziemann, P. J. and Jimenez, J. L.: The 2005 Study of Organic Aerosols at Riverside (SOAR-1): instrumental intercomparisons and fine particle composition, Atmos. Chem. Phys., 11, 12387–12420, doi:10.5194/acp-11-12387-2011, 2011.

Drewnick, F., Hings, S. S., DeCarlo, P., Jayne, J. T., Gonin, M., Fuhrer, K., Weimer, S., Jimenez, J. L., Demerjian, K. L., Borrmann, S. and Worsnop, D. R.: A new Time-of-Flight Aerosol Mass Spectrometer (TOF-AMS)—Instrument description and first field deployment, Aerosol Sci. Technol., 39, 637–658, doi:10.1080/02786820500182040, 2005.

Farmer, D. K., Matsunaga, A., Docherty, K. S., Surratt, J. D., Se- infeld, J. H., Ziemann P. J., and Jimenez, J. L.: Response of an aerosol mass spectrometer to organonitrates and organosulfates and implications for atmospheric chemistry, P. Natl. Acad. Sci. USA, 107, 6670–6675, doi:10.1073/pnas.0912340107, 2010.

Favez, O., El Haddad, I., Piot, C., Boréave, a., Abidi, E., Marchand, N., Jaffrezo, J.-L., Besombes, J.-L., Personnaz, M.-B., Sciare, J., Wortham, H., George, C. and D'Anna, B.: Inter-comparison of source apportionment models for the estimation of wood burning aerosols during wintertime in an Alpine city (Grenoble, France), Atmos. Chem. Phys., 10, 5295–5314, doi:10.5194/acp-10-5295-2010, 2010.

Fry, J. L., Kiendler-Scharr, A., Rollins, A. W., Wooldridge, P. J., Brown, S. S., Fuchs, H., Dubé, W., Mensah, A., dal Maso, M., Tillmann, R., Dorn, H.-P., Brauers, T. and Cohen, R. C.: Organic nitrate and secondary organic aerosol yield from NO_3 oxidation of β-pinene evaluated using a gas-phase kinetics/aerosol partitioning model, Atmos. Chem. Phys., 9, 1431–1449, doi:10.5194/acp-9-1431-2009, 2009.

Fuller, G. W., Sciare, J., Lutz, M., Moukhtar, S. and Wagener, S.: New Directions: Time to tackle urban wood burning?, Atmos. Environ., 68, 295–296, doi:10.1016/j.atmosenv.2012.11.045, 2013.

Fuller, G. W., Tremper, A. H., Baker, T. D., Yttri, K. E. and Butterfield, D.: Contribution of wood burning to PM$_{10}$ in London, Atmos. Environ., 87, 87–94, doi:10.1016/j.atmosenv.2013.12.037, 2014.

Gaidajis, G., Angelakoglou, K. and Aktsoglou, D.: Wintertime particulate mass concentrations in urban environment and the impact of economic crisis., J. Environ. Sci. Health. A. Tox. Hazard. Subst. Environ. Eng., 49, 1653–60, doi:10.1080/10934529.2014.951221, 2014.

Ge, X., Setyan, A., Sun, Y. and Zhang, Q.: Primary and secondary organic aerosols in Fresno, California during wintertime: Results from high resolution aerosol mass spectrometry, J. Geophys. Res., 117, doi:10.1029/2012JD018026, 2012.

Gkatzelis, G. I., Papanastasiou, D. K., Florou, K., Kaltsonoudis, C., Louvaris, E. and Pandis, S. N.: Measurement of nonvolatile particle number size distribution, Atmos. Meas. Tech., 9, 103–114, doi:10.5194/amt-9-103-2016, 2016.

Grantz, D. a, Garner, J. H. B. and Johnson, D. W.: Ecological effects of particulate matter., Environ. Int., 29, 213–39, doi:10.1016/S0160-4120(02)00181-2, 2003.

Hallquist, M., Wenger, J. C., Baltensperger, U., Rudich, Y., Simpson, D., Claeys, M., Dommen, J., Donahue, N. M., George, C., Goldstein, A. H., Hamilton, J. F., Herrmann, H., Hoffmann, T., Iinuma, Y., Jang, M., Jenkin, M. E., Jimenez, J. L., Kiendler-Scharr, A., Maenhaut, W., McFiggans, G., Mentel, T. F., Monod, A., Prévôt, A. S. H., Seinfeld, J. H., Surratt, J. D., Szmigielski, R. and Wildt, J.: The formation, properties and impact of secondary organic aerosol: current and emerging issues, Atmos. Chem. Phys., 9, 5155–5236, doi:10.5194/acp-9-5155-2009, 2009.

Hao, L. Q., Kortelainen, a., Romakkaniemi, S., Portin, H., Jaatinen, a., Leskinen, a., Komppula, M., Miettinen, P., Sueper, D., Pajunoja, a., Smith, J. N., Lehtinen, K. E. J., Worsnop, D. R., Laaksonen, a. and Virtanen, a.: Atmospheric submicron aerosol composition and particulate organic nitrate formation in a boreal forestland–urban mixed region, Atmos. Chem. Phys. Discuss., 14, 17263–17298, doi:10.5194/acpd-14-17263-2014, 2014.

He, L.-Y., Lin, Y., Huang, X.-F., Guo, S., Xue, L., Su, Q., Hu, M., Luan, S.-J. and Zhang, Y.-H.: Characterization of high-resolution aerosol mass spectra of primary organic aerosol emissions from Chinese cooking and biomass burning, Atmos. Chem. Phys., 10, 11535–11543, doi:10.5194/acp-10-11535-2010, 2010.

Heringa, M. F., DeCarlo, P. F., Chirico, R., Tritscher, T., Dommen, J., Weingartner, E., Richter, R., Wehrle, G., Prévôt, a. S. H. and Baltensperger, U.: Investigations of primary and secondary particulate matter of different wood combustion appliances with a high-resolution time-of-flight aerosol mass spectrometer, Atmos. Chem. Phys., 11, 5945–5957, doi:10.5194/acp-11-5945-2011, 2011.

Herndon, S. C., Onasch, T. B., Wood, E. C., Kroll, J. H., Canagaratna, M. R., Jayne, J. T., Zavala, M. a., Knighton, W. B., Mazzoleni, C., Dubey, M. K., Ulbrich, I. M., Jimenez, J.

775   L., Seila, R., de Gouw, J. a., de Foy, B., Fast, J., Molina, L. T., Kolb, C. E. and Worsnop,
          D. R.: Correlation of secondary organic aerosol with odd oxygen in Mexico City,
          Geophys. Res. Lett., 35, L15804, doi:10.1029/2008GL034058, 2008.

Hodzic, A., Jimenez, J. L., Madronich, S., Aiken, A. C., Bessagnet, B., Curci, G., Fast, J.,
          Lamarque, J.-F., Onasch, T. B., Roux, G., Schauer, J. J., Stone, E. A. and Ulbrich, I. M.:
780   Modeling organic aerosols during MILAGRO: importance of biogenic secondary organic
          aerosols, Atmos. Chem. Phys., 9, 6949–6981, doi:10.5194/acp-9-6949-2009, 2009.

Huang, M., Carmichael, G. R., Spak, S. N., Adhikary, B., Kulkarni, S., Cheng, Y., Wei, C.,
          Tang, Y., D'Allura, a., Wennberg, P. O., Huey, G. L., Dibb, J. E., Jimenez, J. L.,
          Cubison, M. J., Weinheimer, a. J., Kaduwela, a., Cai, C., Wong, M., Bradley Pierce, R.,
785   Al-Saadi, J. a., Streets, D. G. and Zhang, Q.: Multi-scale modeling study of the source
          contributions to near-surface ozone and sulfur oxides levels over California during the
          ARCTAS-CARB period, Atmos. Chem. Phys., 11, 3173–3194, doi:10.5194/acp-11-
          3173-2011, 2011.

Jayne, J. T., Leard, D. C., Zhang, X., Davidovits, P., Smith, K. A., Kolb, C. E. and Worsnop,
790   D. R.: Development of an Aerosol Mass Spectrometer for size and composition analysis
          of submicron particles, Aerosol Sci. Technol., 33, 49–70, doi:10.1080/027868200410840,
          2000.

Jimenez, J. L., Canagaratna, M. R., Donahue, N. M., Prevot, A. S. H., Zhang, Q., Kroll, J. H.,
          DeCarlo, P. F., Allan, J. D., Coe, H., Ng, N. L., Aiken, a C., Docherty, K. S., Ulbrich, I.
795   M., Grieshop, A. P., Robinson, A. L., Duplissy, J., Smith, J. D., Wilson, K. R., Lanz, V.
          A., Hueglin, C., Sun, Y. L., Tian, J., Laaksonen, a, Raatikainen, T., Rautiainen, J.,
          Vaattovaara, P., Ehn, M., Kulmala, M., Tomlinson, J. M., Collins, D. R., Cubison, M. J.,
          Dunlea, E. J., Huffman, J. A., Onasch, T. B., Alfarra, M. R., Williams, P. I., Bower, K.,
          Kondo, Y., Schneider, J., Drewnick, F., Borrmann, S., Weimer, S., Demerjian, K.,
800   Salcedo, D., Cottrell, L., Griffin, R., Takami, A., Miyoshi, T., Hatakeyama, S., Shimono,
          A., Sun, J. Y., Zhang, Y. M., Dzepina, K., Kimmel, J. R., Sueper, D., Jayne, J. T.,
          Herndon, S. C., Trimborn, A. M., Williams, L. R., Wood, E. C., Middlebrook, A. M.,
          Kolb, C. E., Baltensperger, U. and Worsnop, D. R.: Evolution of organic aerosols in the
          atmosphere., Science, 326, 1525–9, doi:10.1126/science.1180353, 2009.

805   Kaltsonoudis, C., Kostenidou, E., Florou, K., Psichoudaki, M., and Pandis, S. N.: Temporal
          variability and sources of VOCs in urban areas of Eastern Mediterranean, Atmos. Chem.
          Phys. Discuss., doi:10.5194/acp-2016-358, 2016.

Kanakidou, M., Seinfeld, J. H., Pandis, S. N., Barnes, I., Dentener, F. J., Facchini, M. C., Van
          Dingenen, R., Ervens, B., Nenes, a., Nielsen, C. J., Swietlicki, E., Putaud, J. P.,
810   Balkanski, Y., Fuzzi, S., Horth, J., Moortgat, G. K., Winterhalter, R., Myhre, C. E. L.,
          Tsigaridis, K., Vignati, E., Stephanou, E. G. and Wilson, J.: Organic aerosol and global
          climate modelling: a review, Atmos. Chem. Phys., 5, 1053–1123, doi:10.5194/acp-5-
          1053-2005, 2005.

815 Katragkou, E., Kazadzis, S., Amiridis, V., Papaioannou, V., Karathanasis, S. and Melas, D.: PM_{10} regional transport pathways in Thessaloniki, Greece, Atmos. Environ., 43, 1079–1085, doi:10.1016/j.atmosenv.2008.11.021, 2009.

Kostenidou, E., Pathak, R. K. and Pandis, S. N.: An algorithm for the calculation of secondary organic aerosol density combining AMS and SMPS Data, Aerosol Sci. Technol., 41, 1002–1010, doi:10.1080/02786820701666270, 2007.

820 Kostenidou, E., Lee, B.-H., Engelhart, G. J., Pierce, J. R. and Pandis, S. N.: Mass spectra deconvolution of low, medium, and high volatility biogenic secondary organic aerosol., Environ. Sci. Technol., 43, 4884–9, 2009.

Kostenidou, E., Kaltsonoudis, C., Tsiflikiotou, M., Louvaris, E., Russell, L. M. and Pandis, S. N.: Burning of olive tree branches: a major organic aerosol source in the Mediterranean, 825 Atmos. Chem. Phys., 13, 8797–8811, doi:10.5194/acp-13-8797-2013, 2013.

Kostenidou, E., Florou, K., Kaltsonoudis, C., Tsiflikiotou, M., Vratolis, S., Eleftheriadis, K. and Pandis, S. N.: Sources and chemical characterization of organic aerosol during the summer in the eastern Mediterranean, Atmos. Chem. Phys., 15, 11355–11371, doi:10.5194/acp-15-11355-2015, 2015.

830 Koulouri, E., Saarikoski, S., Theodosi, C., Markaki, Z., Gerasopoulos, E., Kouvarakis, G., Makela, T., Hillamo, R. and Mihalopoulos, N.: Chemical composition and sources of fine and coarse aerosol particles in the Eastern Mediterranean, Atmos. Environ., 42, 6542–6550, doi:10.1016/j.atmosenv.2008.04.010, 2008.

Kroll, J. H., Donahue, N. M., Jimenez, J. L., Kessler, S. H., Canagaratna, M. R., Wilson, K. R., 835 Altieri, K. E., Mazzoleni, L. R., Wozniak, A. S., Bluhm, H., Mysak, E. R., Smith, J. D., Kolb, C. E. and Worsnop, D. R.: Carbon oxidation state as a metric for describing the chemistry of atmospheric organic aerosol., Nat. Chem., 3, 133–9, doi:10.1038/nchem.948, 2011.

Langford, B., Davison, B., Nemitz, E. and Hewitt, C. N.: Mixing ratios and eddy covariance 840 flux measurements of volatile organic compounds from an urban canopy (Manchester, UK), Atmos. Chem. Phys., 9, 1971–1987, doi:10.5194/acp-9-1971-2009, 2009.

Lanz, V. a, Alfarra, M. R., Baltensperger, U., Buchmann, B., Hueglin, C., Szidat, S., Wehrli, M. N., Wacker, L., Weimer, S., Caseiro, A., Puxbaum, H. and Prevot, A. S. H.: Source attribution of submicron organic aerosols during wintertime inversions by advanced 845 factor analysis of aerosol mass spectra., Environ. Sci. Technol., 42, 214–20, 2008.

Lanz, V. A., Alfarra, M. R., Baltensperger, U., Buchmann, B., Hueglin, C. and Prévôt, A. S. H.: Source apportionment of submicron organic aerosols at an urban site by factor analytical modelling of aerosol mass spectra, Atmos. Chem. Phys., 7, 1503–1522, doi:10.5194/acp-7-1503-2007, 2007.

850 Lelieveld, J., Crutzen, P. J., Ramanathan, V., Andreae, M. O., Brenninkmeijer, C. M., Campos,

855   T., Cass, G. R., Dickerson, R. R., Fischer, H., de Gouw, J. A., Hansel, A., Jefferson, A.,
       Kley, D., de Laat, A. T., Lal, S., Lawrence, M. G., Lobert, J. M., Mayol-Bracero, O. L.,
       Mitra, A. P., Novakov, T., Oltmans, S. J., Prather, K. A., Reiner, T., Rodhe, H., Scheeren,
       H. A., Sikka, D. and Williams, J.: The Indian Ocean experiment: widespread air pollution
       from South and Southeast Asia., Science, 291, 1031–6, doi:10.1126/science.1057103,
       2001.

       Louvaris, E., Florou, K., Karnezi, E., Gkatzelis, G., Papanastasiou, D. and Pandis, S. N.
       Volatility of source apportioned wintertime organic aerosol in the city of Athens, to be
       submitted, 2016.

860   Mohr, C., Huffman, J. A., Cubison, M. J., Aiken, A. C., Docherty, K. S., Kimmel, J. R.,
       Ulbrich, I. M., Hannigan, M. and Jimenez, J. L.: Characterization of primary organic
       aerosol emissions from meat cooking, trash burning, and motor vehicles with High-
       Resolution Aerosol Mass Spectrometry and comparison with ambient and chamber
       observations, Environ. Sci. Technol., 43, 2443–2449, doi:10.1021/es8011518, 2009.

865   Mohr, C., DeCarlo, P. F., Heringa, M. F., Chirico, R., Slowik, J. G., Richter, R., Reche, C.,
       Alastuey, a., Querol, X., Seco, R., Peñuelas, J., Jiménez, J. L., Crippa, M., Zimmermann,
       R., Baltensperger, U. and Prévôt, a. S. H.: Identification and quantification of organic
       aerosol from cooking and other sources in Barcelona using aerosol mass spectrometer
       data, Atmos. Chem. Phys., 12, 1649–1665, doi:10.5194/acp-12-1649-2012, 2012.

870   Murphy, B. N., Donahue, N. M., Fountoukis, C. and Pandis, S. N.: Simulating the oxygen
       content of ambient organic aerosol with the 2D volatility basis set, Atmos. Chem. Phys.,
       11, 7859–7873, doi:10.5194/acp-11-7859-2011, 2011.

       Nel, A.: Atmosphere. Air pollution-related illness: effects of particles., Science, 308, 804–806,
       doi:10.1126/science.1108752, 2005.

875   Ng, N. L., Kwan, A. J., Surratt, J. D., Chan, A. W. H., Chhabra, P. S., Sorooshian, A., Pye, H.
       O. T., Crounse, J. D., Wennberg, P. O., Flagan, R. C. and Seinfeld, J. H.: Secondary
       organic aerosol (SOA) formation from reaction of isoprene with nitrate radicals (NO_3),
       Atmos. Chem. Phys., 8, 4117–4140, doi:10.5194/acp-8-4117-2008, 2008.

       Paatero, P. and Tapper, U.: Positive matrix factorization: A non-negative factor model with
880   optimal utilization of error estimates of data values, Environmetrics, 5, 111–126,
       doi:10.1002/env.3170050203, 1994.

       Paraskevopoulou, D., Liakakou, E., Gerasopoulos, E., Theodosi, C. and Mihalopoulos, N.:
       Long-term characterization of organic and elemental carbon in the $PM_{2.5}$ fraction: the
       case of Athens, Greece, Atmos. Chem. Phys., 14, 13313–13325, doi:10.5194/acp-14-
885   13313-2014, 2014.

       Petrakakis, M.J.; Kelessis, A.G.; Tzoumaka, P.; Samara, C. (2013). Levels of Suspended
       Particulate Matter before and after the Economic Crisis in Thessaloniki, Greece,

Proceedings of 17th International Symposium on Environmental Pollution and its Impact on Life in the Mediterranean Region, Istanbul, Turkey, Sept 28–Oct 1, 2013. Mediterranean Scientific Association of Environmental Protection (MESAEP).

Petzold, A. and Schönlinner, M.: Multi-angle absorption photometry—a new method for the measurement of aerosol light absorption and atmospheric black carbon, J. Aerosol Sci., 35, 421–441, doi:10.1016/j.jaerosci.2003.09.005, 2004.

Pikridas, M., Tasoglou, A., Florou, K. and Pandis, S. N.: Characterization of the origin of fine particulate matter in a medium size urban area in the Mediterranean, Atmos. Environ., 80, 264–274, doi:10.1016/j.atmosenv.2013.07.070, 2013.

Puxbaum, H., Caseiro, A., Sánchez-Ochoa, A., Kasper-Giebl, A., Claeys, M., Gelencsér, A., Legrand, M., Preunkert, S. and Pio, C.: Levoglucosan levels at background sites in Europe for assessing the impact of biomass combustion on the European aerosol background, J. Geophys. Res., 112, D23S05, doi:10.1029/2006JD008114, 2007.

Robinson, A. L., Subramanian, R., Donahue, N. M., Bernardo-Bricker, A. and Rogge, W. F.: Source apportionment of molecular markers and organic aerosol. 3. Food Cooking Emissions, Environ. Sci. Technol., 40, 7820–7827, doi:10.1021/es060781p, 2006.

Rollins, A. W., Kiendler-Scharr, A., Fry, J. L., Brauers, T., Brown, S. S., Dorn, H.-P., Dubé, W. P., Fuchs, H., Mensah, A., Mentel, T. F., Rohrer, F., Tillmann, R., Wegener, R., Wooldridge, P. J. and Cohen, R. C.: Isoprene oxidation by nitrate radical: alkyl nitrate and secondary organic aerosol yields, Atmos. Chem. Phys., 9, 6685–6703, doi:10.5194/acp-9-6685-2009, 2009.

Saarikoski, S., Carbone, S., Decesari, S., Giulianelli, L., Angelini, F., Canagaratna, M., Ng, N. L., Trimborn, a., Facchini, M. C., Fuzzi, S., Hillamo, R. and Worsnop, D.: Chemical characterization of springtime submicrometer aerosol in Po Valley, Italy, Atmos. Chem. Phys., 12, 8401–8421, doi:10.5194/acp-12-8401-2012, 2012.

Sage, A. M., Weitkamp, E. A., Robinson, A. L. and Donahue, N. M.: Evolving mass spectra of the oxidized component of organic aerosol: results from aerosol mass spectrometer analyses of aged diesel emissions, Atmos. Chem. Phys., 8, 1139–1152, doi:10.5194/acp-8-1139-2008, 2008.

Schauer, J. J. and Cass, G. R.: Source apportionment of wintertime gas-phase and particle-phase air pollutants using organic compounds as tracers, Environ. Sci. Technol., 34, 1821–1832, doi:10.1021/es981312t, 2000.

Schneider, J., Hock, N., Weimer, S., Borrmann, S., Kirchner, U., Vogt, R. and Scheer, V.: Nucleation particles in diesel exhaust: composition inferred from in situ mass spectrometric analysis., Environ. Sci. Technol., 39, 6153–61, 2005.

Stein, S. E. and Scott, D. R.: Optimization and testing of mass spectral library search algorithms for compound identification, 1994.

925   Steinbacher, M., Dommen, J., Ammann, C., Spirig, C., Neftel, A. and Prevot, A. S. H.: Performance characteristics of a proton-transfer-reaction mass spectrometer (PTR-MS) derived from laboratory and field measurements, Int. J. Mass Spectrom., 239, 117–128, doi:10.1016/j.ijms.2004.07.015, 2004.

Stohl, a., Forster, C., Frank, A., Seibert, P. and Wotawa, G.: Technical note: The Lagrangian
930   particle dispersion model FLEXPART version 6.2, Atmos. Chem. Phys., 5, 2461–2474, doi:10.5194/acp-5-2461-2005, 2005.

Sueper, D.: ToF-AMS High Resolution Analysis Software – Pika, online available at: http://cires.colorado.edu/jimenez-group/ ToFAMSResources/ToFSoftware, 2011.

Sullivan, a. P., Holden, a. S., Patterson, L. a., McMeeking, G. R., Kreidenweis, S. M., Malm,
935   W. C., Hao, W. M., Wold, C. E. and Collett, J. L.: A method for smoke marker measurements and its potential application for determining the contribution of biomass burning from wildfires and prescribed fires to ambient $PM_{2.5}$ organic carbon, J. Geophys. Res., 113, D22302, doi:10.1029/2008JD010216, 2008.

Sun, Y. L., Zhang, Q., Schwab, J. J., Chen, W.-N., Bae, M.-S., Hung, H.-M., Lin, Y.-C., Ng, N.
940   L., Jayne, J., Massoli, P., Williams, L. R. and Demerjian, K. L.: Characterization of near-highway submicron aerosols in New York City with a high-resolution aerosol mass spectrometer, Atmos. Chem. Phys., 12, 2215–2227, doi:10.5194/acp-12-2215-2012, 2012.

Sun, Y.-L., Zhang, Q., Schwab, J. J., Demerjian, K. L., Chen, W.-N., Bae, M.-S., Hung, H.-M.,
945   Hogrefe, O., Frank, B., Rattigan, O. V. and Lin, Y.-C.: Characterization of the sources and processes of organic and inorganic aerosols in New York city with a high-resolution time-of-flight aerosol mass apectrometer, Atmos. Chem. Phys., 11, 1581–1602, doi:10.5194/acp-11-1581-2011, 2011.

Theodosi, C., Grivas, G., Zarmpas, P., Chaloulakou, a. and Mihalopoulos, N.: Mass and
950   chemical composition of size-segregated aerosols (PM_1, $PM_{2.5}$, PM_{10}) over Athens, Greece: local versus regional sources, Atmos. Chem. Phys., 11, 11895–11911, doi:10.5194/acp-11-11895-2011, 2011.

Trainer, M. G., Jimenez, J. L., Yung, Y. L., Toon, O. B. and Tolbert, M. a: Nitrogen incorporation in CH_4-N_2 photochemical aerosol produced by far ultraviolet irradiation.,
955   Astrobiology, 12, 315–26, doi:10.1089/ast.2011.0754, 2012.

Turpin, B. J. and Huntzicker, J. J.: Identification of secondary organic aerosol episodes and quantitation of primary and secondary organic aerosol concentrations during SCAQS, Atmos. Environ., 29, 3527–3544, doi:10.1016/1352-2310(94)00276-Q, 1995.

Ulbrich, I. M., Canagaratna, M. R., Zhang, Q., Worsnop, D. R. and Jimenez, J. L.:
960   Interpretation of organic components from Positive Matrix Factorization of aerosol mass spectrometric data, Atmos. Chem. Phys., 9, 2891–2918, doi:10.5194/acp-9-2891-2009, 2009.

Vlasenko, a., Slowik, J. G., Bottenheim, J. W., Brickell, P. C., Chang, R. Y.-W., Macdonald, a. M., Shantz, N. C., Sjostedt, S. J., Wiebe, H. a., Leaitch, W. R. and Abbatt, J. P. D.: Measurements of VOCs by proton transfer reaction mass spectrometry at a rural Ontario site: Sources and correlation to aerosol composition, J. Geophys. Res., 114, D21305, doi:10.1029/2009JD012025, 2009.

Watson, J. G.: Visibility: Science and Regulation, J. Air Waste Manage. Assoc., 52, 628–713, doi:10.1080/10473289.2002.10470813, 2002.

Wotawa, G. and Trainer, M.: The influence of Canadian forest fires on pollutant concentrations in the United States, Science, 288, 324–328, doi:10.1126/science.288.5464.324, 2000.

Zhang, Q., Jimenez, J. L., Canagaratna, M. R., Allan, J. D., Coe, H., Ulbrich, I., Alfarra, M. R., Takami, a., Middlebrook, a. M., Sun, Y. L., Dzepina, K., Dunlea, E., Docherty, K., DeCarlo, P. F., Salcedo, D., Onasch, T., Jayne, J. T., Miyoshi, T., Shimono, a., Hatakeyama, S., Takegawa, N., Kondo, Y., Schneider, J., Drewnick, F., Borrmann, S., Weimer, S., Demerjian, K., Williams, P., Bower, K., Bahreini, R., Cottrell, L., Griffin, R. J., Rautiainen, J., Sun, J. Y., Zhang, Y. M. and Worsnop, D. R.: Ubiquity and dominance of oxygenated species in organic aerosols in anthropogenically-influenced Northern Hemisphere midlatitudes, Geophys. Res. Lett., 34, doi:10.1029/2007GL029979, 2007.

965

970

975

980

Table 1. Coefficient of determination R^2 between the OA factors in Athens and VOCs

m/z	BBOA	HOA	COA	OOA
42 (acetonitrile)	0.81	0.67	0.35	0.20
43	0.71	0.59	0.30	0.19
47 (formic acid)	0.43	0.49	0.11	0.06
59 (acetone, glyoxal)	0.70	0.61	0.31	0.25
61 (acetic acid)	0.52	0.33	0.18	0.14
69 (isoprene, furan)	0.88	0.63	0.31	0.14
71 (MVK, MACR)	0.81	0.74	0.32	0.13
73 (MEK)	0.75	0.61	0.31	0.21
75 (hydroxyacetone)	0.69	0.41	0.24	0.09
79 (benzene)	0.71	0.70	0.31	0.16
81 (terpenes)	0.85	0.63	0.30	0.15
85 (EVK)	0.90	0.68	0.34	0.14
87 (MBO, C5, methacrylic acid)	0.93	0.59	0.33	0.15
93 (toluene)	0.37	0.54	0.18	0.09
95 (2 vinyl furan, phenol)	0.43	0.36	0.12	0.02
99 (hexenal)	0.87	0.58	0.34	0.21
101 (isoprene hyperoxides)	0.71	0.48	0.25	0.12
105 (styrene)	0.54	0.55	0.19	0.09
107 (xylenes)	0.47	0.65	0.23	0.11
113 (chlorobenzene)	0.80	0.53	0.31	0.21
115 (heptanal)	0.66	0.48	0.22	0.13
121 (C9 aromatics)	0.47	0.66	0.21	0.10
129 (octanal, naphthalene)	0.70	0.73	0.21	0.07
135 (C10 aromatics)	0.50	0.64	0.21	0.12
137 (monoterpenes)	0.71	0.52	0.25	0.19
139 (nopinone)	0.67	0.41	0.22	0.18
151 (pinonaldehyde)	0.32	0.26	0.09	0.06
163 (C12 aromatics)	0.38	0.27	0.10	0.12

985
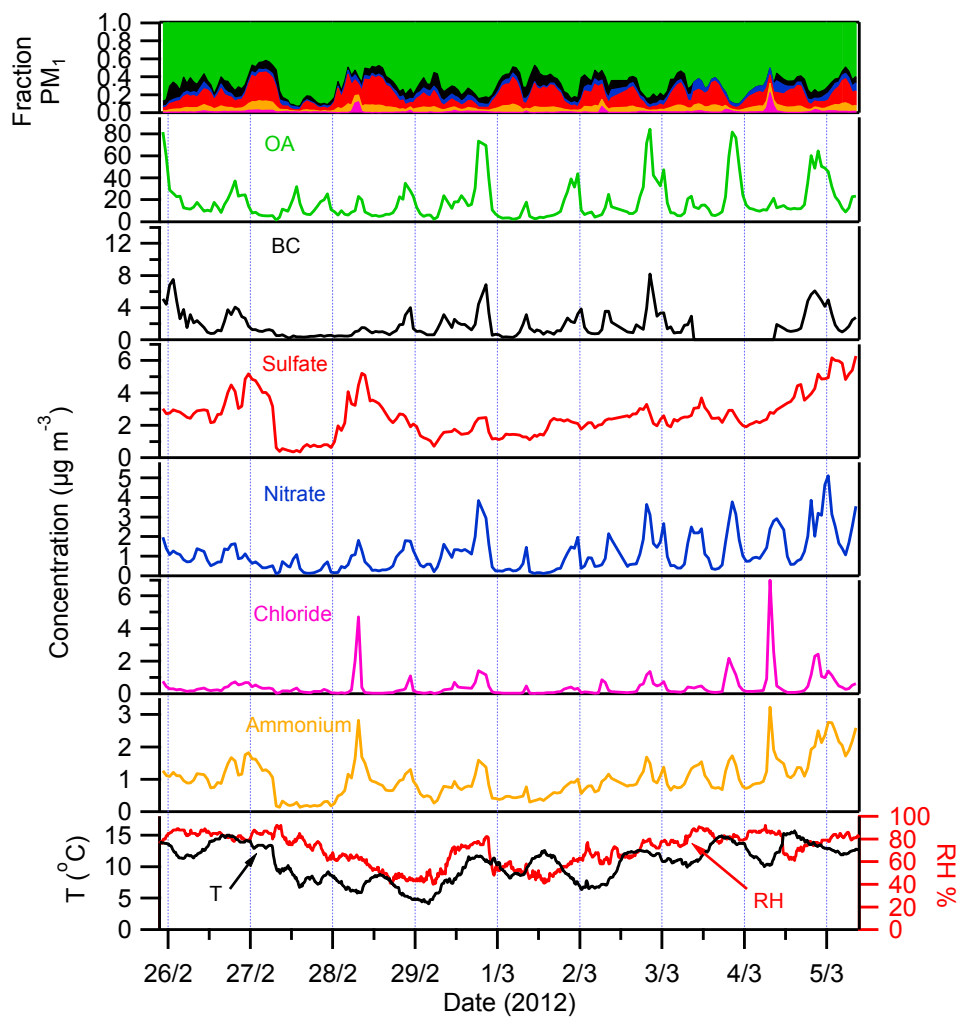
Figure 1. Fractional contribution and time series (hourly averages) of the main PM$_1$ species during the Patras campaign. Also shown the temperature and RH.
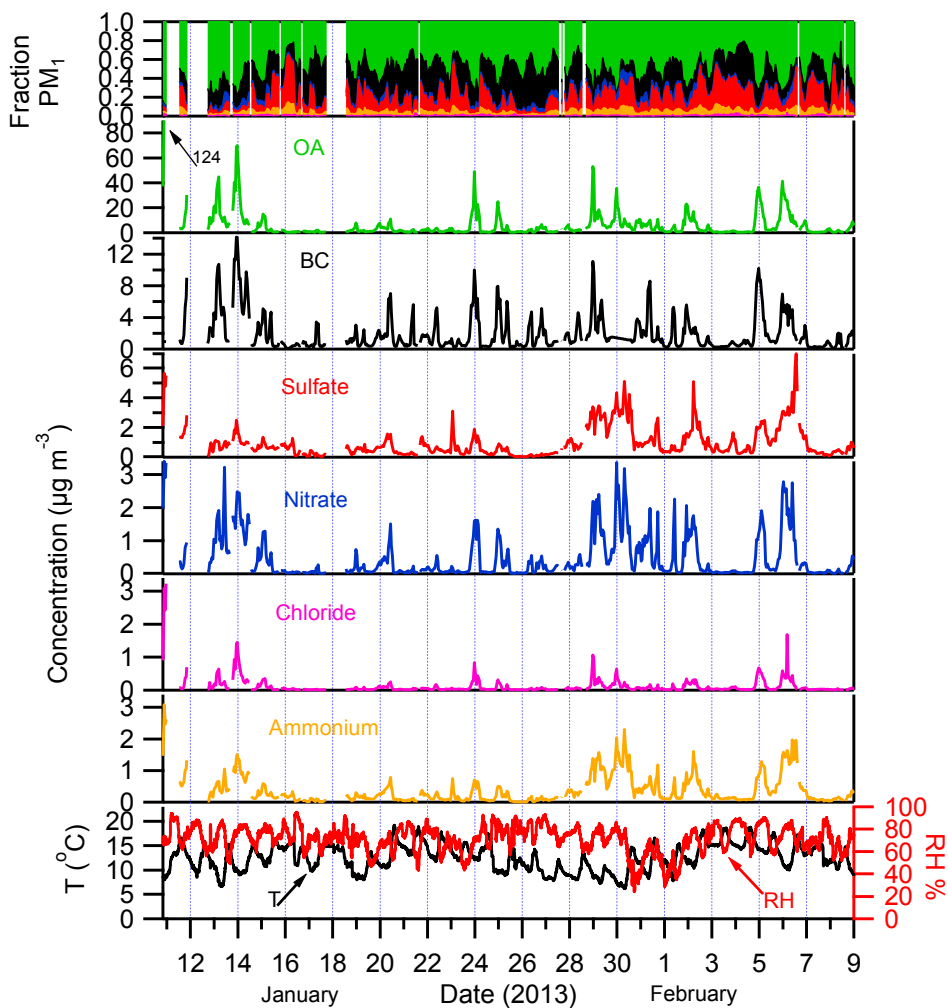
Figure 2. Fractional contribution and time series (hourly averages) of the main PM$_1$ species during the Athens campaign. Also shown the temperature and RH.
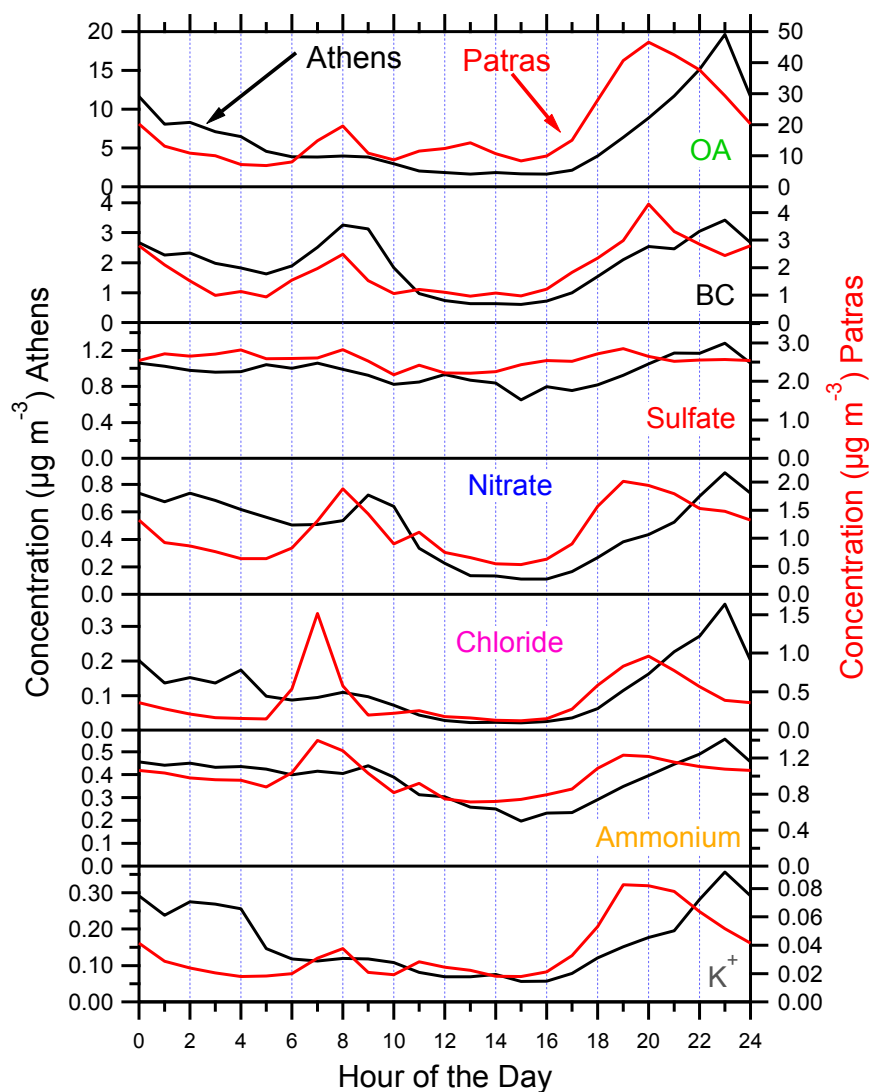
Figure 3. Average diurnal profiles for the main PM_1 components during the Athens and Patras

995   campaigns. The concentration of PM_1 in Patras is shown in the right y-axis.
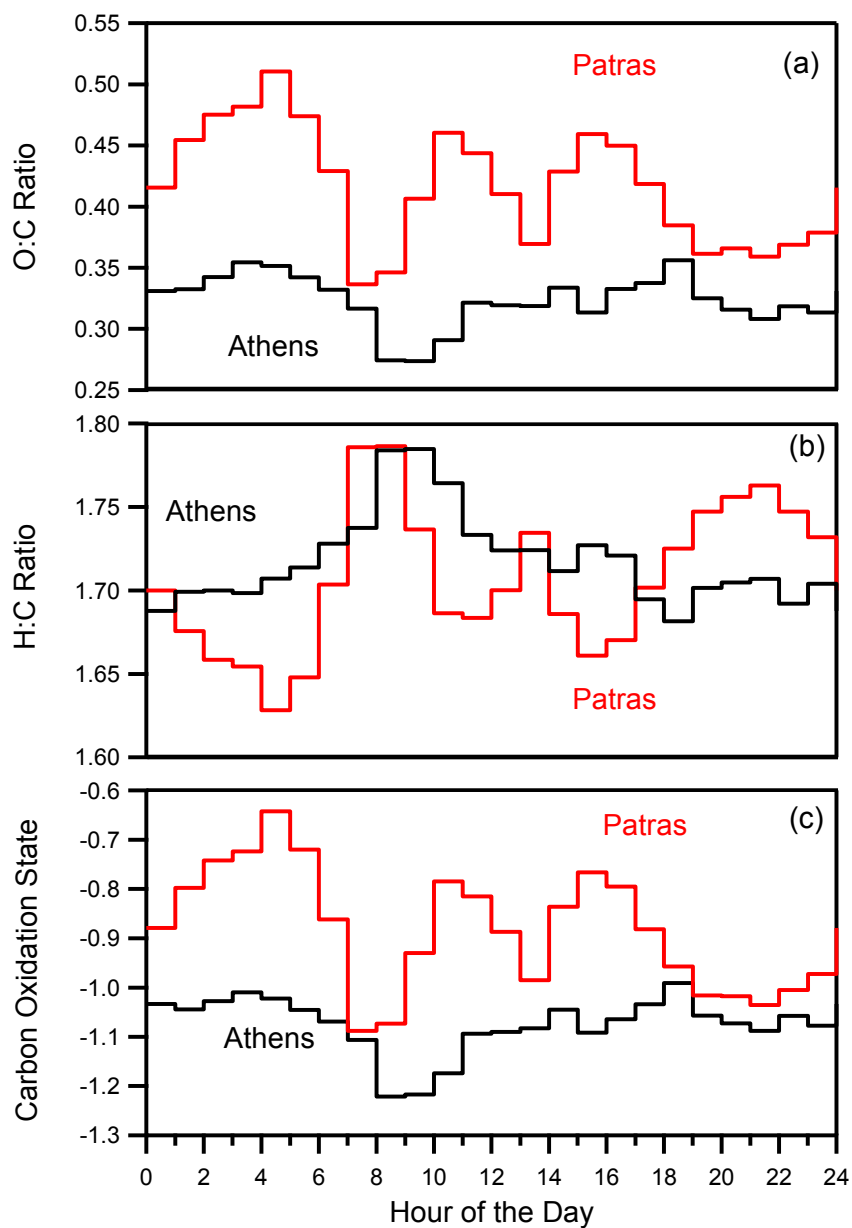
Figure 4. The diurnal profile of (a) the O:C ratio; (b) the H:C ratio; and (c) the OS$_C$ in Athens (black) and Patras (red). The ratios have been calculated following the Canagaratna et al. (2015) approach.

1000
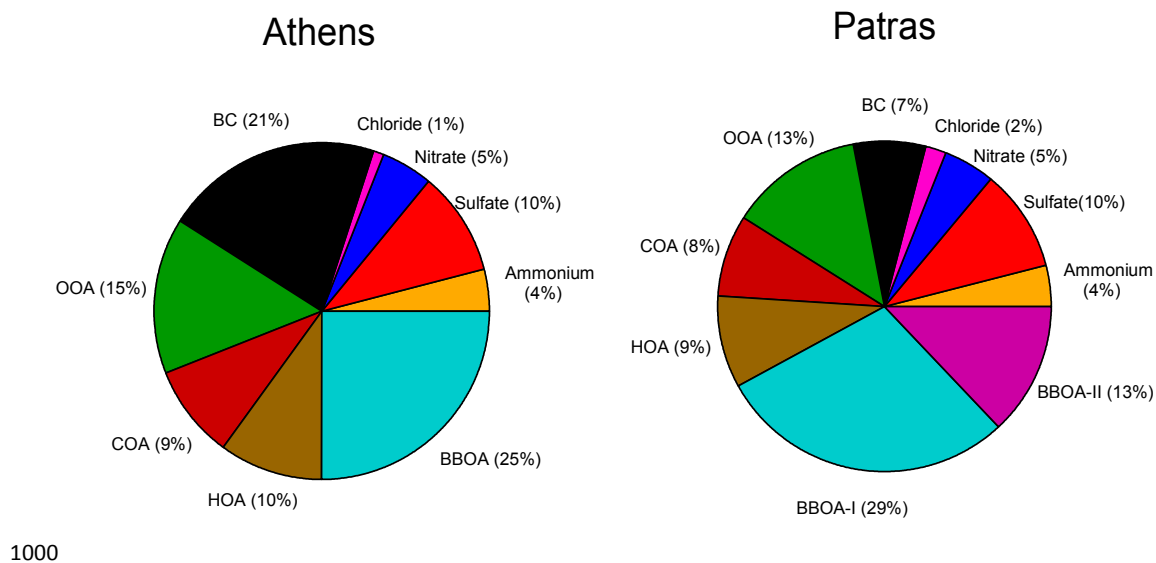
Figure 5. Average PM$_1$ composition and organics source apportionment for Athens and Patras. The average PM$_1$ for Athens was 10 µg m^{-3} while for Patras 25 µg m^{-3}.
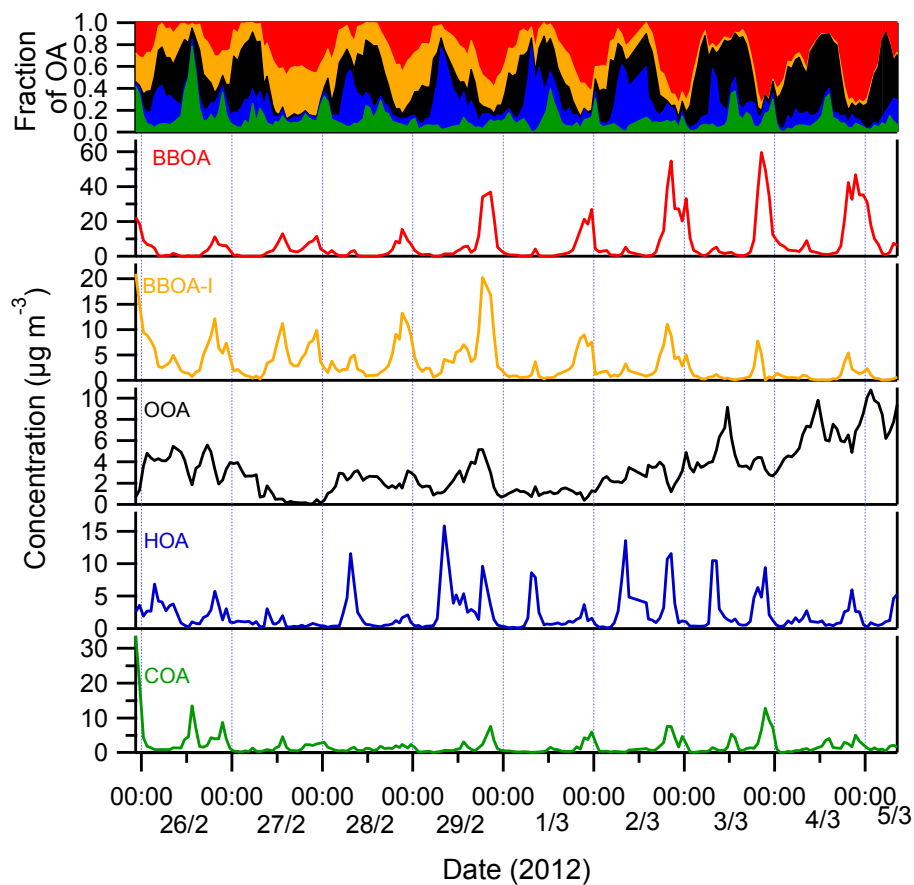
1005

Figure 6. Fractional contribution to OA and time series of the PMF factors during the Patras campaign.
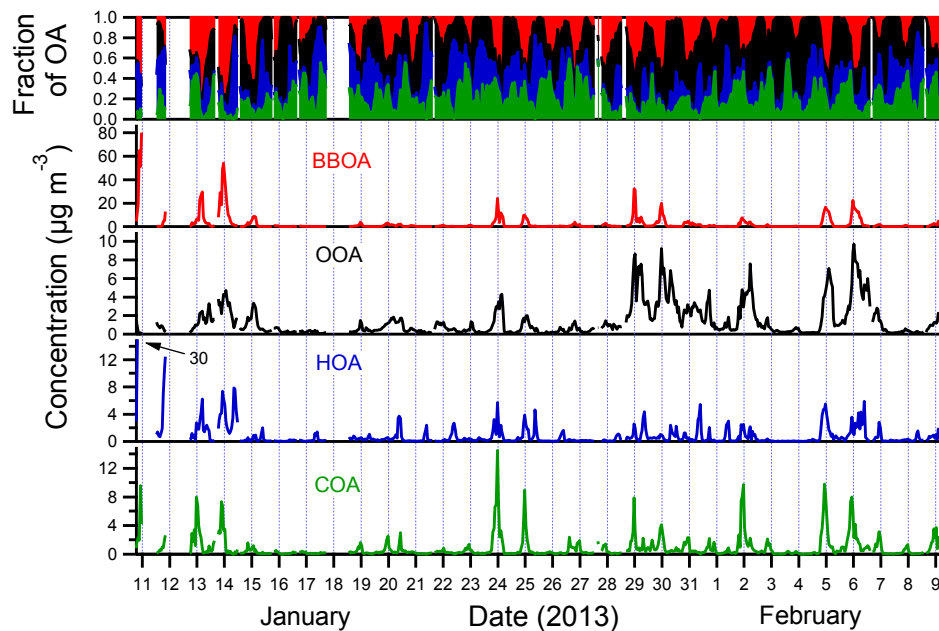
1010

Figure 7. The hourly fractional contribution to OA and time series of the PMF factors during the Athens campaign.
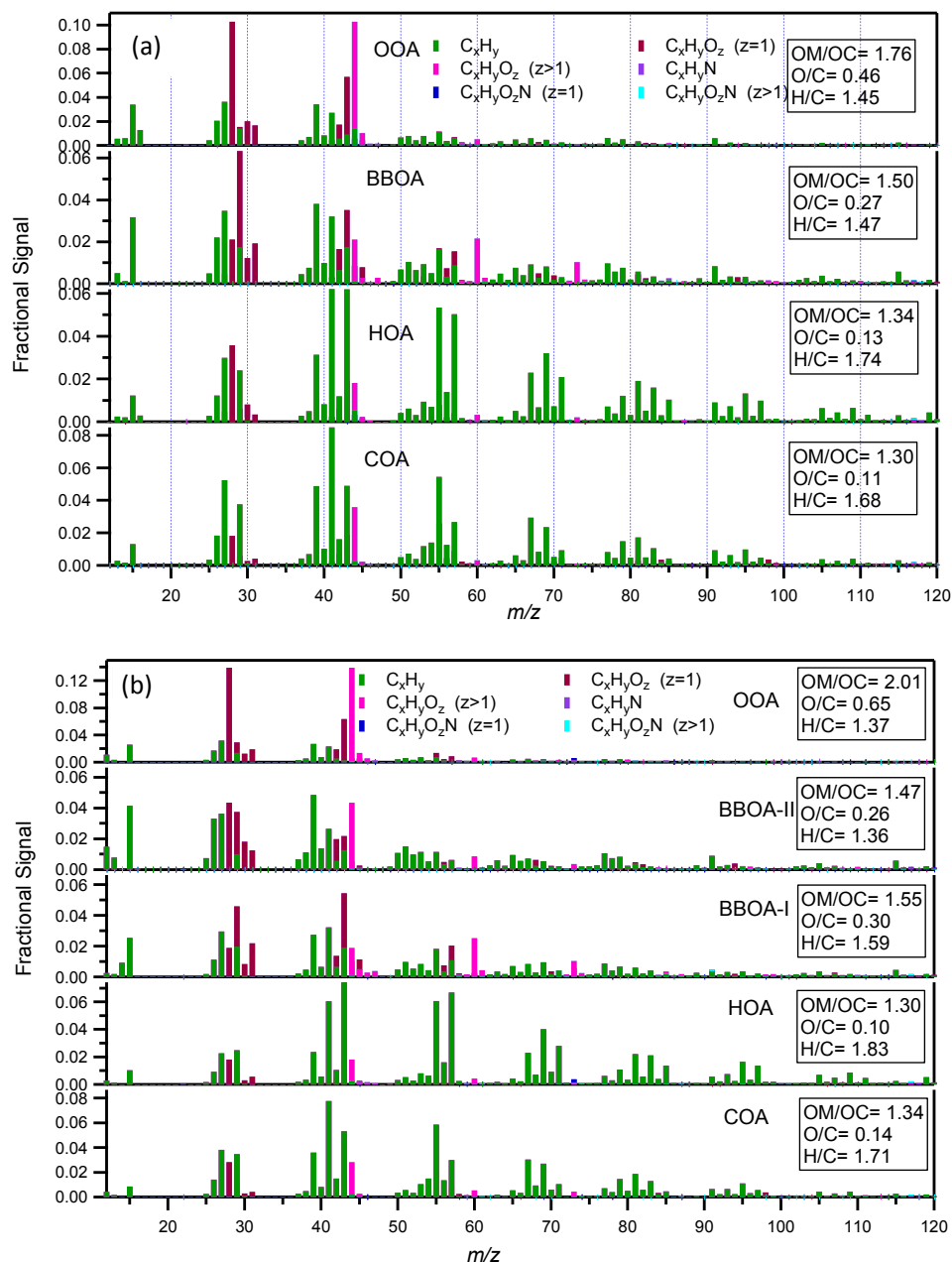
Figure 8. High resolution AMS mass spectra for the factors in (a) Athens and (b) Patras.
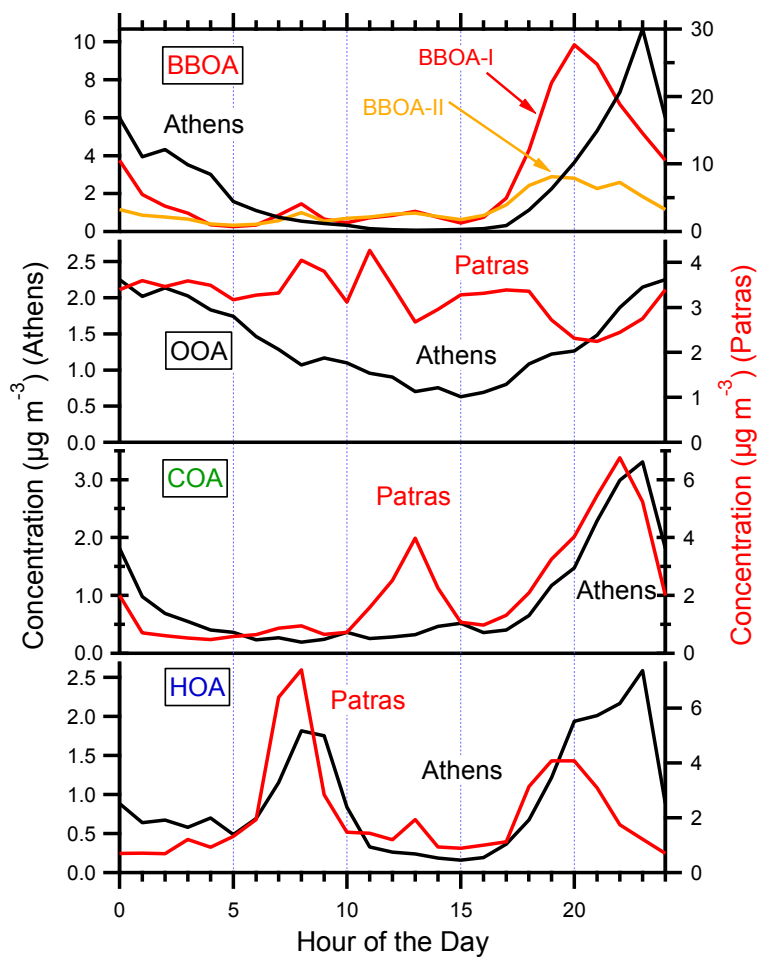
Figure 9. Diurnal profiles of the PMF factors in Athens (black) and Patras (red-yellow). On the
left y-axis are the concentrations of Athens' PMF factors, while on the right y-axis those of
Patras.